D.6.1.4 - Methodology and specification report for static model analysis - Theoretical concepts and Analysis Procedure (M45 version)

WP6.1 - Static model analysis

WP6 - Modelling and simulation services

MODRIO (11004)

Version 2.0
Date 18/04/2016

Authors Toufik Bentaleb CNRS-Ampère
Minh Tu Pham CNRS-Ampère
Wilfrid Marquis-Favre CNRS-Ampère

Executive summary

This report is the 2nd report of the deliverable D6.1.4 of task WP6.1 [1]. One of the goals of this task is to extend the techniques already in use for the physical structural analysis of mechatronics systems to perform static analysis and diagnosis on physical models in order to state whether they are well-posed and suitable for each step of the system's lifecycle (from its design to its operation). If a problem for modeling, for simulating or for solving the given engineering question is detected, the analysis shall localize the problem in the model and give the physical interpretation of the error. The objective is not to be able to diagnose all possible physical errors, but to add another type of analysis in order to improve error detection before compiling and running a model.

The approach proposed by the laboratory Ampère is intended to answer to the industrial needs described in the deliverables D6.1.1 [2] and D6.1.2 [3] (Intermediate cooling system -SRI- for EDF nuclear plants, Environmental Control System -ECS- for Dassault-Aviation and, vehicle dynamics applications for Siemens-LMSInternational). It should also bring complementary tools to the approaches presented in the deliverable D6.1.3 by Siemens-LMS-International [4].

The first report of this deliverable [5] has presented the basic concepts for the physical structural analysis, the criteria for the structural invertibility verification and the mathematical differentiability conditions for the output specifications. This second report presents a transcription of the SRI model (EDF) into a bond graph representation, its physical structural analysis and some specifications for undertaking this analysis in Modelica language.

Summary

1. Introduction

Physical structural analysis should be viewed as complementary to numerical simulation but a valuable model-based approach for giving information about how far a model is suitable to answer to an engineering problem (model inversion, input reconstruction, control input synthesis, state estimation, parameter identification,...) Interestingly enough, by its nature physical structural analysis is undertaken before simulation and even before the model source compiling. It is the step just after fixing the assumptions and both the energy architecture and the phenomena behavior laws of the system model. The first great interest of physical structural analysis is that it relates the model capability features to answer to an engineering problem with the physical system information. A second interest is that when the properties or the criteria are not satisfied at this stage, it is not needed to pursue an useless numerical analysis. A third interest is that the physical structural analysis gives guidelines to where and how to reformulate the model for it to suit the engineering problem when some criteria are not satisfied.

The task undertaken by the laboratory Ampère in the MODRIO project was, in collaboration with its Workpackage 6 partners, to first demonstrate the capability of the physical structural analysis to apply on industrial use-cases. This step has necessitated to transcript partners' models into the original graphic language for which the physical structural analysis was prescribed. This graphic language is bond graph [6]. Then some analyses have been applied on the bond graph representation with the objective to translate them back to the model original language, namely Modelica. The work presented lies on the concepts presented in the first report of this deliverable [5].

The following section presents the Intermediary Cooling System (French acronym Système de Réfrigération Intermédiaire or SRI) and a simplified version on which the physical structural analysis is later undertaken. The details of the Modelica model and the bond graph model of SRI are given in Section 3. Its physical structural analysis both at a local component level and a global system level are also provided. Section 4 presents an illustration of the physical structural analysis used for the example of state estimation in the heat exchanger of SRI. Finally Section 5 presents the very first specifications of Modelica language for integrating the concepts and some procedure bricks of the physical structural analysis into that language.

2. Use-case presentation: SRI

2.1. General description

The SRI is a cooling subsystem used in nuclear power plants. It is composed of 4 sub-systems (Figure 1):

- the cooling system, with two heat exchangers, two regulation valves, and a by-pass valve,
- the water circulation system, made of 3 pumps (in parallel) and three check valves,
- the water feeding system with a feeding tank,
- the auxiliary equipment standing for the load of the system with a source of heat and a user valve.

In addition, there are three control main functions:

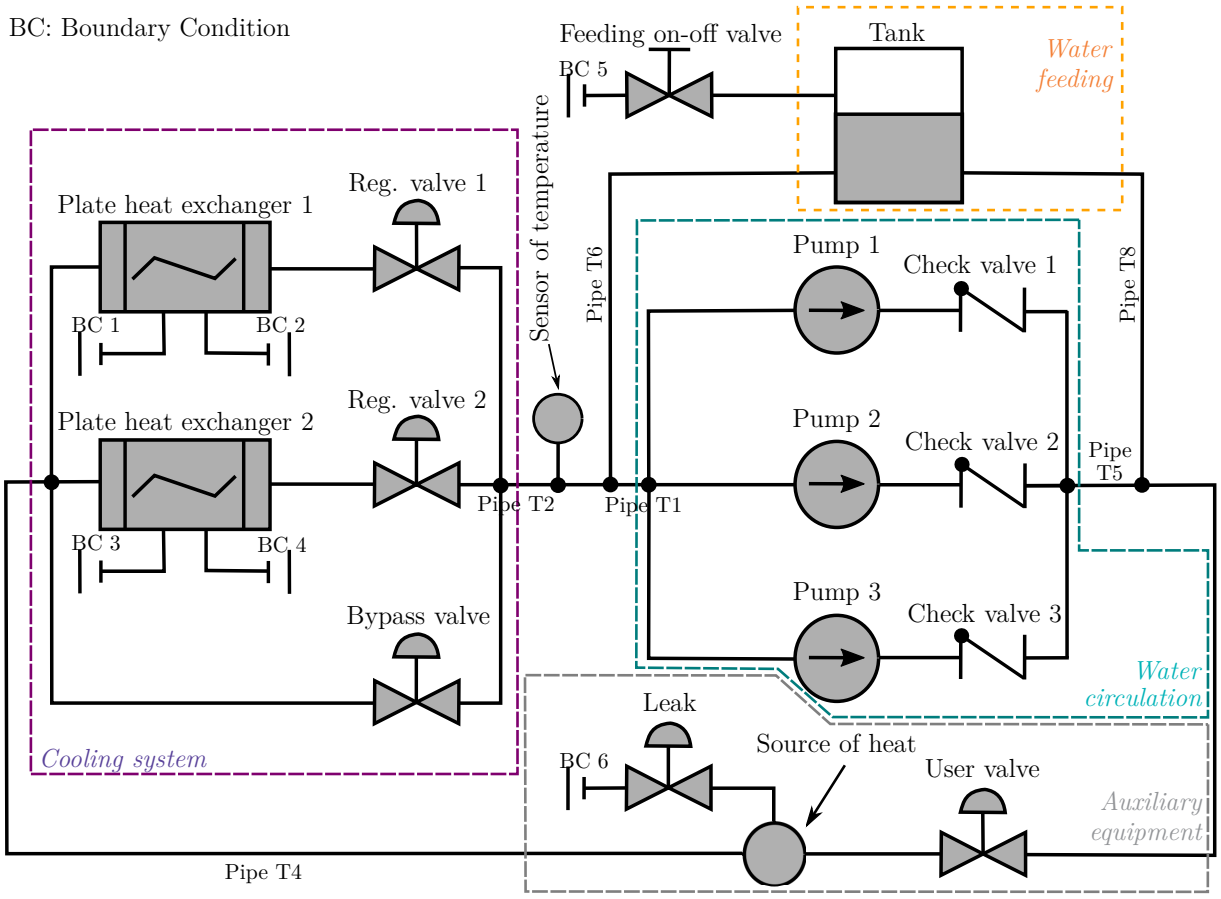

Figure 1: Schematic description of the SRI

- the control of the temperature set point at the outlet of the heat exchangers (analog controller for the regulations valves),
- the control of the tank water level between two bounds (on-off controller),
- the control of the startup of the backup pump.

2.2. Model simplification

In order to demonstrate the interest of the physical structural analysis and to clearly see the specifications of the Modelica language from this task, it has been decided to work on a simplified version of the SRI (Figure 2).

Only the components of the nominal functioning mode have been retained. The following parts have been discarded:

- the bypass valve of the cooling system,
- the pump and its check valve that are emergency components for the water circulation,
- the controllers.

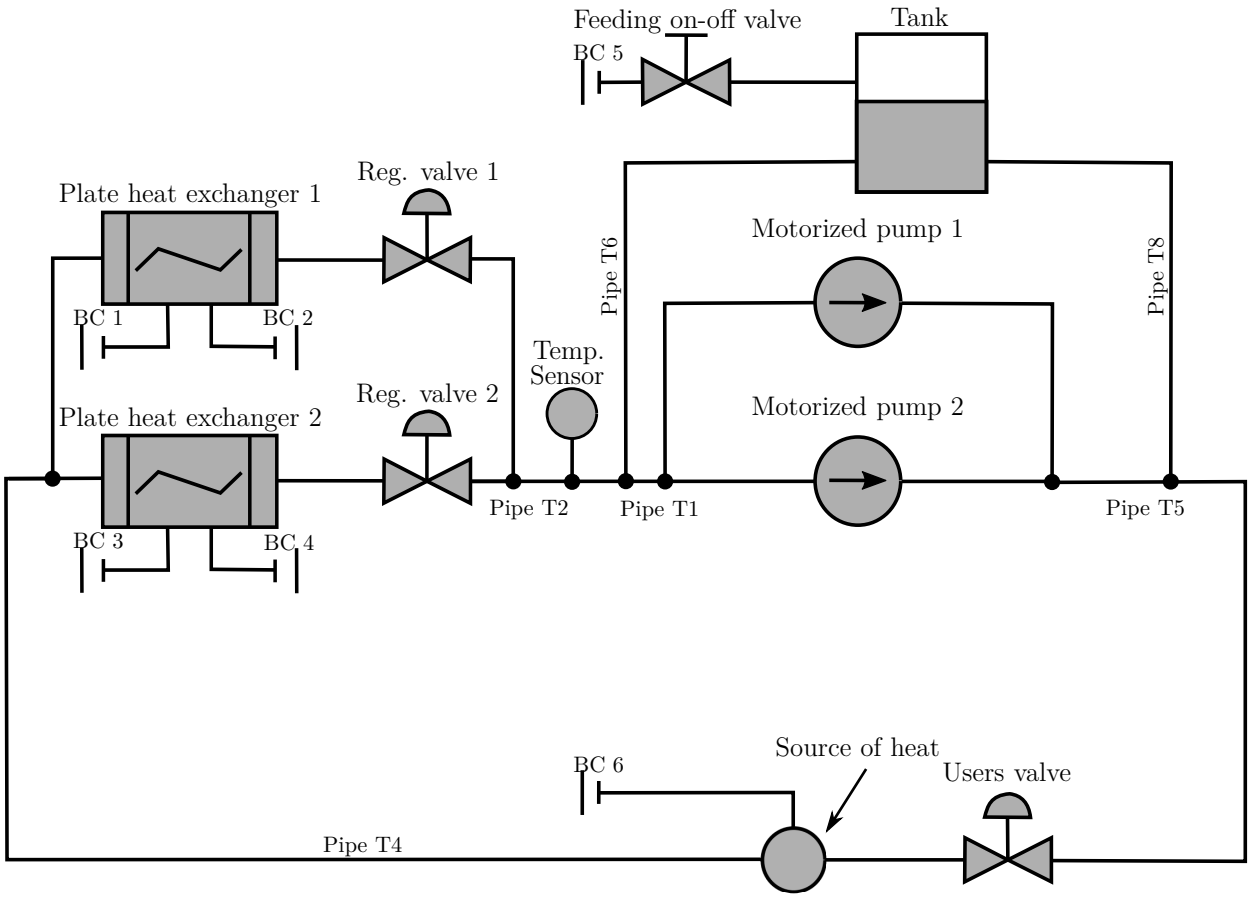

Figure 2: Schematic description of the simplified SRI

Furthermore the following assumptions are considered:

- the heat intake is given,
- the valves opening are given (users' valve),
- the initial fluid height in the feeding tank is known and never goes down under the outlet orifice,
- the orifice diameters in the feeding tank are not taken into account,
- all the pressure and temperature boundary conditions are given,
- there is no water flow inversion in any part of the circuit (so no need of check valves),
- there is no water flow threshold effect,
- there is no change of water phase which stays liquid,
- there is no leak in the auxiliary equipment.

The boundary condition values of SRI are given in Table 1 of Appendix A.1.

3. Structural Physical analysis of SRI

This section first presents the component models in Modelica language, in bond graph and a local phase of physical structural analysis. Then the bond graph of the complete model is presented by connection of the previous component representations and a global structural analysis is undertaken. The component Modelica models belong to the ThermosysPro library [7, 8, 9, 10, 11]. This open source library, developed by EDF R&D, is used to model energy systems and different types of power plants (nuclear, conventional, solar, etc.) [12]. The complete Modelica model is developed in Dymola [13].

3.1. Local phase: component level

The local phase aims at working out important results on the structure properties at the component level. This shall lead to identify the state variables that are to be initialized at this level and the other variables that should be determined from these state variables. This phase shall also show input and output variables avoiding as possible algeabric loops at the component level or otherwise how to break them. The results given during local phase of analysis must be kept to indicate how to address physical structural issues at the system level of analysis. Section 3.2.2 will illustrate this feature.

Structural physical analysis is undertaken at this level for the SRI. For each component, the Modelica model is first given.

3.1.1. heat exchanger

Modelica model

The plate heat exchanger is the component that transforms heat (thermal energy) from one fluid to another. Plate heat exchangers have a high heat transfer rate compared to other types of heat exchangers due to their large surface area. The dynamic water/water heat exchanger component used belongs to the ThermoSysPro library. The core model of the heat exchanger was written in Modelica and simulated with the Dymola simulation environment. Figure 3 shows the schematic of the heat exchanger model in Dymola. This model has two parts: the upper part for hot water and the other part for cold water, which are quite similar. The inlets and outlets of the heat exchanger block are shown by the blue and red rectangles, respectively. The red and blue arrows show the cold and hot waters of the two parts respectively.

A pictorial representation of the discretized counterflow heat exchanger is shown in Figure 4. The modeling is based on a finite volume approach where each lump is associated to a control volume. Figure 5 shows one volume with its adjacent neighbors and the different attached variables as well as the variables "flowing" through the boundaries or the pressure drops between two volumes.

In this Modelica model, the rate of mass accumulation within a volume does not incorporate any dynamic effects. This means that the entering mass flow rate is exactly equal to the leaving one i.e. the steady balance for all volumes of the heat exchanger, yields:

$$q_{b,i-1} - q_{b,i} = 0 \qquad \forall i \in \{2; \ldots; N\} \tag{1}$$

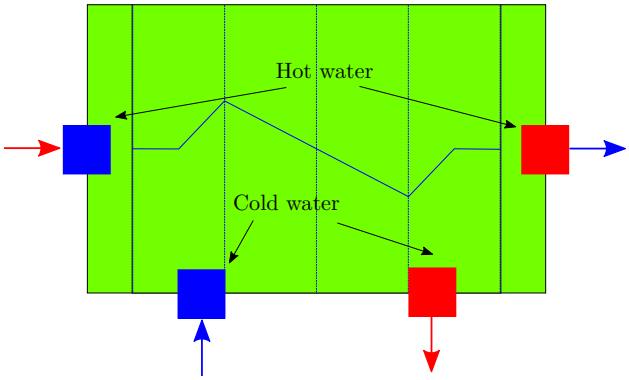

Figure 3: Dymola layout of the heat exchanger.

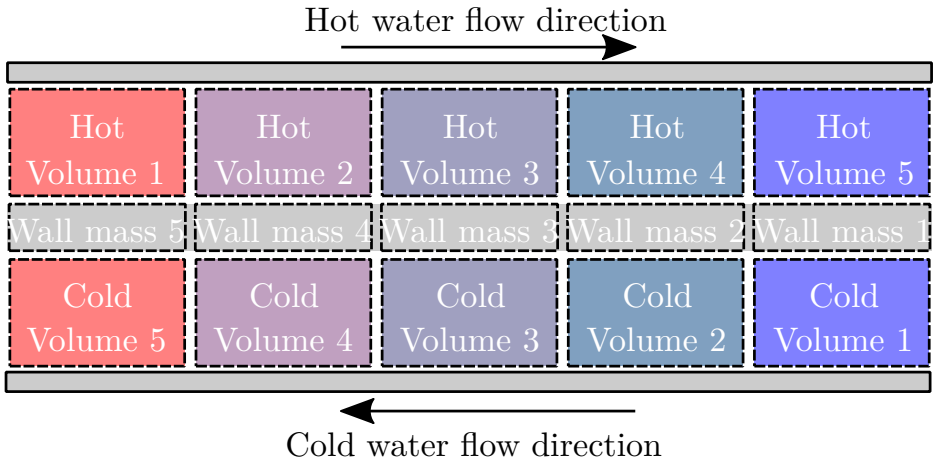

Figure 4: Schematic diagram of a typical 5 lumps discretized counterflow plate heat exchanger.

where N is the number of segments, q the mass flow rate and the subscript b means the hot branch when ($b \to h$) or the cold branch when ($b \to c$).

The pressure relationship between two adjacent volumes is defined by:

$$P_{b,I} = P_{b,I-1} - \Delta P_{b,i}/N \qquad \forall i \in \{1; \ldots; N-1\} \text{ and } \forall I \in \{1; \ldots; N\} \tag{2}$$

where $\Delta P_{b,i} = \Delta P_{b,i}\left(q_{b,i}, \mu_{b,i}, \rho_{b,i}\right)$ is the pressure drop, $\mu_{b,i}$ the dynamic viscosity, $\rho_{b,i}$ the water density at the boundary i, and i and I are subscripts dedicated to variables respectively at the boundaries and in the volumes (details of the equations are given in Table 2 of Appendix A.2.1).

The water properties for the pressure drop calculation are given by:

$$\begin{cases} \rho_{b,i} = \rho_{b,i}\left(P_{mb,i}, h_{b,I}\right) \\ \mu_{b,i} = \mu_{b,i}\left(\rho_{b,i}, T_{b,I}\right) \end{cases} \tag{3}$$

where $h_{b,I}$ is the water specific enthalpy in the control volume, $T_{b,I} = T_{b,I}\left(P_{mb,i}, h_{b,I}\right)$ is the water temperature and $P_{mb,i}$ is the averaged pressure between two volumes:

$$P_{mb,i} = \frac{P_{b,I-1} + P_{b,I}}{2} \tag{4}$$

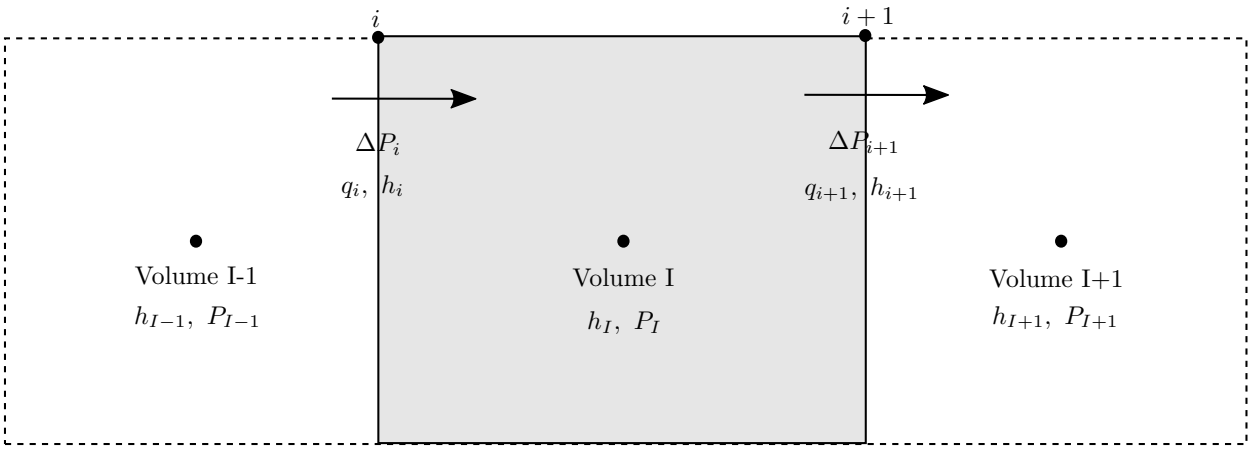

Figure 5: Staggered finite volume scheme

The energy balance equations in each control volume of each branch is given by:

$$V_{b,I} \cdot \rho_{b,I} \cdot \frac{\mathrm{d}h_{b,I}}{\mathrm{d}t} = q_{b,i} \cdot h_{b,I} - q_{b,i+1} \cdot h_{b,I+1} \pm \dot{W}_I \tag{5}$$

where the plus sign (+) stands for the hot branch and the minus sign (-) for the cold one, $V_{b,I}$ is the volume of a control volume, and $\rho_{b,I}$ is the water density.

The global heat exchanged between the both fluids and the wall is

$$\dot{W}_I = K_I \cdot \Delta S \cdot (T_{h,I} - T_{c,I}) \tag{6}$$

Where ΔS is the heat exchange surface, $K_I = K_I\left(q_{h,i}, q_{c,i}, \mu_{h,I}, \mu_{c,I}, Cp_{h,I}, Cp_{c,I}, \lambda_{h,I}, \lambda_{c,I}\right)$ is the global heat transfer coefficient, $Cp_{b,I}$ is the water heat capacity and $\lambda_{b,I}$ is the water thermal conductivity (details are given in Appendix A.2.1).

The water properties are given here by:

$$\begin{cases} T_{b,I} = T_{b,I}\left(P_{b,I}, h_{b,I}\right) \\ \rho_{b,I} = \rho_{b,I}\left(P_{b,I}, h_{b,I}\right) \\ \mu_{b,I} = \mu_{b,I}\left(\rho_{b,I}, T_{b,I}\right) \\ Cp_{b,I} = Cp_{b,I}(P_{b,I}, h_{b,I}) \\ \lambda_{b,I} = \lambda_{b,I}\left(\rho_{b,I}, T_{b,I}, P_{b,I}\right) \end{cases} \tag{7}$$

The functions in Equations (3) and (7) of the water properties are based on the Industrial Formulation IAPWS-IF97 which consists of a set of equations for different water regions (more details are given in [14]).

The paremeters of the heat exchangers are given in Table 2 of Appendix A.1.

Bond graph model

In the literature, bond graph modelling of heat exchangers is widespread [15, 16, 17]. Due to difficulties in handling entropy and heat transfer rate, many efforts have been made to develop pseudo-bond graph representations of thermo-fluid transport and heat exchange [18, 19, 20, 21, 22]. All these references mentioned above have different assumptions. For instance, in [15] a temperature-entropy bond graph technique has been proposed based on three lump models to predict the reversal of flow. In this model, the authors have considered that the fluid domain is operated independently from the thermal domain. In [19], pseudo bond graph strategies have been proposed with the temperature and heat flow as effort and flow.

In this report the bond graph modelling of the heat exchanger is also based on the finite volume discretization of the branches (Figure 6). It uses the pseudo-bond graph variables in particular in the thermal domain where the conjugated effort- and flow-like variables are the temperature (true effort variable) and the specific enthalpy flow rate (pseudo-flow variable) respectively. This pseudo-bond graph approach will be adopted to the whole SRI modelling throughout this report.

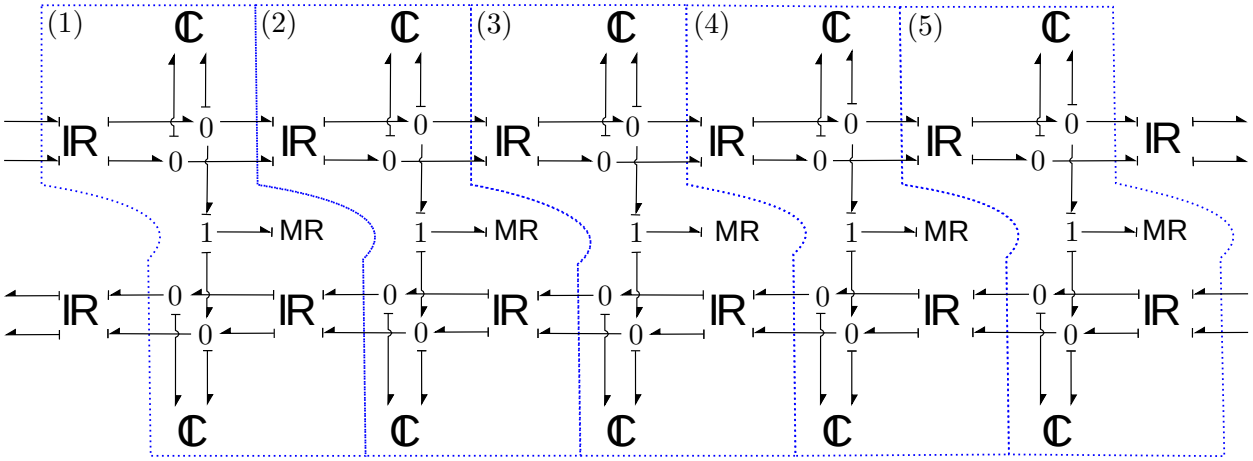

Figure 6: Bond graph representation of a heat exchanger

2-port C-elements

Figure 6 displays two-port C-elements (ℂ) used as thermofluidic accumulators that stands for the energy storage phenomenon in each control volume. A two-port C-element has two energetic degrees of freedom since its volume is fixed here. The two state variables are generalized displacements: the water mass (m) for the fluid domain, and the specific enthalpy (h) for the thermal domain (see Figure 7)[1]. The outputs from the multi-port C-element are the pressure for the fluid port and temperature for the thermal domain. They are given in terms of the state variables and the corresponding functions constitute the behavior laws ot the C-element:

$$\begin{cases} P_I = P_I(\rho_I, h_I) \\ T_I = T_I(P_I, h_I) \end{cases} \tag{8}$$

[1] In this part all the developments are valid for both hot and cold branches. Consequently the corresponding subscripts are voluntary omitted except where otherwise necessary.

where the temperature table $T_I(P_I, h_I)$, thermodynamic property of the water, is well detailed in reference [14] and the ThermoSysPro model.

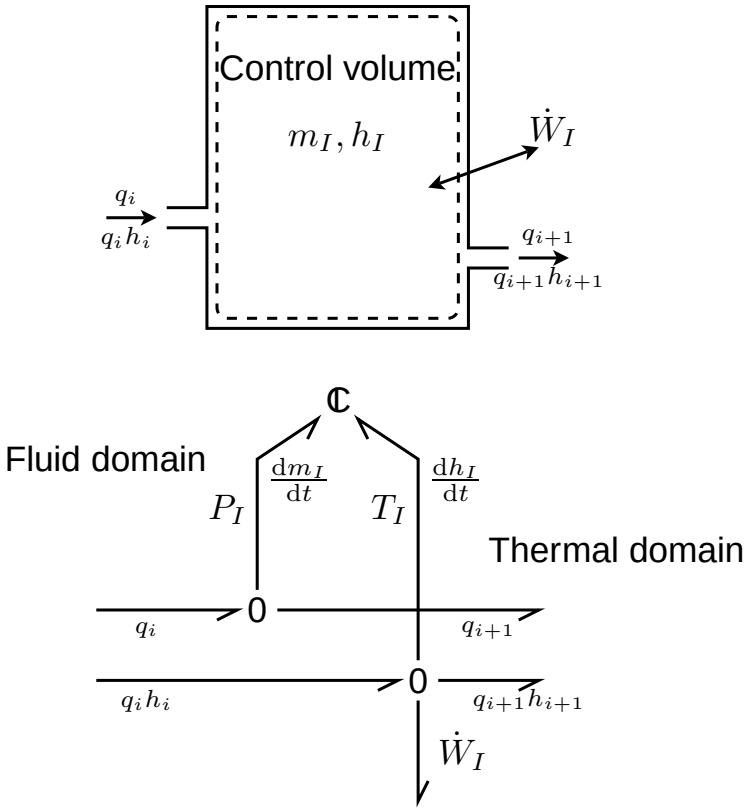

Figure 7: Control volume and its corresponding thermofluidic bond graph representation

Unlike the Modelica model the function $P_I(\rho_I, h_I)$ requires to invert the table of the water density with respect to the pressure. This is calculated by an iterative resolution given in Algorithm 1 described in Appendix A.3. The algorithm provides an easy way to obtain the pressure, as a function of a given density and specific enthalpy.

Then the both 0-junctions are associated to the conservation laws. The left-hand side 0-junction corresponds to the mass conservation that ideally[2] provides the energy storage phenomena with the time derivative of the control volume mass. It is determined from the net balance of the mass flow rate at the boundaries of the control volume as expressed by:

$$\frac{\mathrm{d}m_I}{\mathrm{d}t} = q_i - q_{i+1} \tag{9}$$

where m_I is the mass, q_i and q_{i+1} are mass flow rates at the boundaries, as shown in Figure 7 on the upper horizontal bonds.

Alternatively, if a uniform density is assumed in the control volume, Equation (9) can be converted into a form where the density becomes the state variable:

$$\rho_I = \frac{m_I}{V_I} \tag{10}$$

[2]Here using the adverb "ideally" corresponds to have the ports of this storage phenomena in integral causality.

where V_I is the volume of the control volume.

Assuming a constant and equal volume for each control volume leads to:

$$\frac{\mathrm{d}\rho_I}{\mathrm{d}t} = \frac{q_i - q_{i+1}}{V_I} \tag{11}$$

The right-hand side 0-junction of Figure 7 bond graph is attached to the energy conservation law Equation (12). Assuming a nearly incompressible fluid in the control volume, it furnishes the time derivative of water specific enthalpy to the energy storage phenomenon from a net balance between the specific enthalpy flow rates at the boundaries and the heat flow rate through the exchanger wall:

$$V_I \cdot \rho_I \cdot \frac{\mathrm{d}h_I}{\mathrm{d}t} = q_i \cdot h_i \ - q_{i+1} \cdot h_{i+1} \pm \dot{W}_I \tag{12}$$

the sign $\pm$ in Equations (12) depends on whether the energy conservation law concerns the hot or cold branch.

Multiport R-elements

The Multi-port R-element is used as a thermofluidic resistance at the boundary between two control volumes. The detail of the port variables is given Figure 8. With respect to the ideal causality of both the adjacent control volumes (Figure 7), this element receives the effort variables (pressures P_{I-1} and P_I, and temperatures T_{I-1} and T_I) to furnish in return the mass flow rates q_i and the specific enthalpy flow rates $q_i h_i$ to both adjacent control volumes.

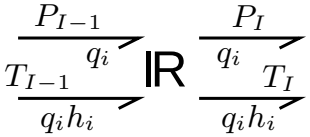

Figure 8: The pseudo bond graph of the R-field of the heat exchanger

The relationships between these effort- and pseudo-flow variables constitute the behavior laws of the multiport R-element and should, due the ideal causality consequences, have the forms:

$$\begin{cases} q_i = q_i(T_{I-1}, T_I, P_{I-1}, P_I) \\ q_i \cdot h_i = q_i \cdot h_i(T_{I-1}, T_I, P_{I-1}, P_I) \end{cases} \tag{13}$$

To calculate the mass flow rate q_i as a function, for one, of the pressure drop $\Delta P_i = P_{I-1} - P_I$ is quite difficult using Equation (40) in Appendix A.2.1. Therefore the pressure drop ΔP_i is first rewritten as:

$$\Delta P_i = k_i \cdot Nu_i^{-0.097} \cdot qu_i^2 + 104.97 \cdot Nu_i^{-0.25} \tag{14}$$

where k_i is expressed by:

$$k_i = 14423.2 \cdot [1472.47 + 1.54 \cdot (M-1)/2] \cdot \frac{c_1}{\rho_i} \tag{15}$$

and the Nusselt number Nu_i, qu_i, M, and c_1 are presented in Appendix A.2.1.

In Equation (14) it is shown that the second term $104.97 \cdot (Nu_{b,i})^{-0.25}$ can be neglected to some extent, at least in the range of the pressure drop variation encountered here in simulation (see Appendix A.4.1). The pressure drop can thus be approximated by:

$$\begin{aligned} \Delta\bar{P}_i &= k_i \cdot Nu_i^{-0.097} \cdot qu_i^2 \\ &= k_i \cdot \left(\frac{q_i}{\mu_i \cdot M}\right)^{-0.097} \cdot \left(\frac{q_i}{M}\right)^2 \\ &= \bar{k}_i \cdot q_i^{2-0.097} \end{aligned} \tag{16}$$

where $\bar{k}_i = k_i \cdot \mu_i^{0.097} \cdot M^{(0.097-2)}$. Finally the mass flow rate q_i can easily be expressed by:

$$q_i = \exp\left(\frac{\ln\left(\Delta\bar{P}_i\right) - \ln\left(\bar{k}_i\right)}{2 - 0.097}\right) \tag{17}$$

Once the mass flow rate is obtained from the pressure drop, it must be multiplied by the specific enthalpy to obtained the specific enthalpy flow rate in Equation (13). Here, the water specific enthalpy as some other properties must be obtained from tables depending on pressure and temperature [14].

Modulated R-elements

The rate of heat transfer in each segment of the heat exchanger occurs between the two corresponding control volumes respectively from the hot and the cold branches. The heat flow $\dot{W}_I$ furnished to the right-hand side 0-junction is proportional to the difference of temperatures and exactly follows the Modelica model (Equation (6)):

$$\dot{W}_I = K_I \cdot \Delta S \cdot (T_{h,I} - T_{c,I}) \tag{18}$$

where K_I is given by Equation (42). It is a function of the convection heat transfer coefficients $\overline{h}_b$ that depend on variables external of the R-element. This justifies its modulation that is materialized by the blue arrows in Figure 9.

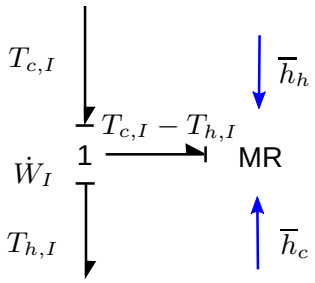

Figure 9: Modulated 1-port R-element and 1-junction

The bond graph model of the exchanger has been validated in simulation (see Appendix A.4.2).

Analysis

As a starting point for the heat exchanger, each step of the bond graph model presentation showed valuable features for a physical structural analysis at this component level. In particular

it has been indicated for the 2-port energy storage phenomenon that the "ideal" causality is an integral causality (Figure 10). In consequence, the causality for the whole heat exchanger model could be assigned indicating how the different behavior laws for the dissipation phenomena (at the boundaries between the control volumes or for the heat exchange between the both hot and cold branches) had to be causally oriented. This has also imposed to use the water property tables in a specific way. This was the case for the density table that has been inverted with respect to the pressure.

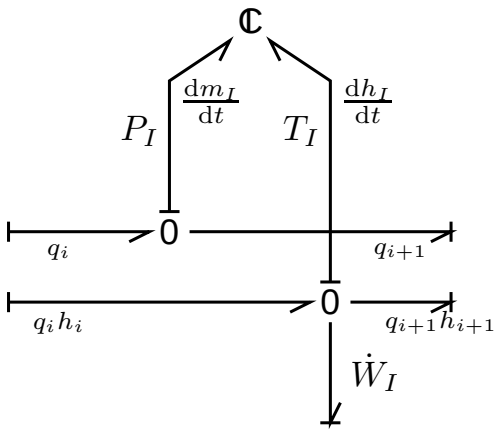

Figure 10: Causal bond graph of a control volume

Of course one may decide to not respect the integral causality for the energy storage phenomenon. The drawback of accepting that is most probably to face simulation difficulties since this would exhibit an useless DAE system that can be otherwise avoided.

Furthermore a careful investigation of the causality on the whole heat exchanger causal model (Figure 6) shows that no algebraic loop is present at this component level. In fact any causal path that would exhibit an algebraic loop from potential R-elements or meshes in the representation goes through the energy storage phenomena by the flow (mass flow rates) or pseudo-flow (specific enthalpy flow rates or heat rates) variables. This means means that the corresponding equation system is an ODE.

Unlike the bond graph model the Modelica model assumes a steady state flow all along the exchanger branches which has as a consequence to suppress a power port on the storage phenomenon on one hand, and to change the causality for the dissipation phenomena on the other hand. By a careful investigation of the series of relationships constituting the behavior law of the dissipation phenomena one can notice the following "cycle" in the variables:

$$P_{b,I} \overset{(2)}{\leftarrow} \Delta P_{b,i} \overset{(40)}{\leftarrow} \rho_{b,i} \overset{(3)}{\leftarrow} P_{mb,i} \overset{(4)}{\leftarrow} P_{b,I}$$

where the arrows stand for "is needed to algebraically compute with the equation above". For instance Equation (2) needs the value of $\Delta P_{b,i}$ to calculate $P_{b,I}$.

This variable cycle, which is a causal path closing on itself, is called a causal loop. Its peculiarity is that its order is equal to 0 meaning that no integration occurs in the series of relationships. In this zero order causal loop the pressures inside the volumes are determined by the mean of the

pressures at the boundaries of the volume. Then the pressures in the volume are used to calculate a mean pressure at a boundary that determines back through the pressure drop law the pressures in the volumes. This is typically an algebraic loop that may cause difficulties and even obstacles to solve the overall model. It is even worse for the whole exchanger model since this situation applies for each lump in each branch.

Different solutions may address the problem of algebraic loop like implicit numerical method used by the solver or index reduction undertaken by the model compiler. However these solutions are not guaranteed and the modeler may even wish his model not having such algebraic loop. Here the physical structural analysis can bring valuable information on how to address this issue at the physical model level. In fact the one undertaken on the bond graph model naturally brought a solution.

The bond graph model presentation showed a port for the storage phenomena on which the time derivative of the control volume mass is determined by the net balance of the mass flow rate (mass conservation law). This rehabilitates an unsteady flow in the exchanger. If it is steady, this will be determined by the functioning conditions and not by an *a priori* assumption. Then the pressure in a control volume is to be determined from the water properties and this is the price to pay here. This requires to invert the $\rho = \rho(P, h)$ water property table with respect to the pressure. Another consequence is to invert the behavior law of pressure drop at control volume boundaries for it to give the mass flow rate in terms of the both pressures imposed by the adjacent control volumes.

Finallly it is worthwhile to note that the bond graph model presented for the heat exchanger has no obstacle, in principle, to address fluid flow inversion without modifying the presented equations or introducing conditional different forms of the equations except for the heat flow through the exchanger wall that depends on the inlet mass flow rate Equation (6). Nevertheless this flow inversion management is *a priori* localized only here instead of on the whole exchanger model. This means that the structure of this model equations intrinsically remains the same in case of flow inversion. This is strongly associated to the causality symmetry of each lump, symmetry that can be viewed as a physical structure property once again.

3.1.2. Feeding tank

Modelica model

The feeding tank prevents the lack of water in the cooling main circuit. The iconic representation of the feeding tank in Dymola is presented Figure 11.

The corresponding model is principally described by the following equations where the different parameters are shown in Table 3 of Appendix A.1.

The mass balance equation is:

$$\rho \cdot A \cdot \frac{\mathrm{d}z}{\mathrm{d}t} = \sum_{i=1}^{2} q_{in,i} - q_{out} \tag{19}$$

where ρ is the water density considered here as constant, A the tank cross sectional area, z the water height, and q_j the mass flow rate with j the subscript indicating the orifice "from feeding

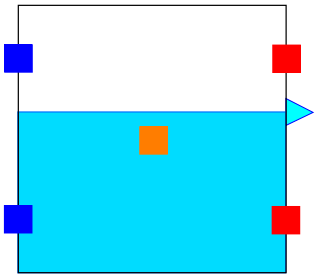

Figure 11: Dymola layout of the feeding tank.

valve" $(in, 1)$, "from tube 6" $(in, 2)$ or "to tube 8" (out).

The energy balance equation is:

$$\rho \cdot A \cdot z \cdot \frac{\mathrm{d}h}{\mathrm{d}t} = \sum_{i=1}^{2} q_{in,i} \cdot (h_{in,i} - h) - q_{out} \cdot (h_{out} - h) \tag{20}$$

where h is the water specific enthalpy.

Inlet and outlet orifices are modeled as singular pressure drops, modulated by the height of water relative to the height of the orifice. The assumptions done for the simplified version of the SRI model enable the following relationship to be written:

$$k \cdot \frac{q_i \cdot |q_i|}{2\rho} = P_{atm} + \rho \cdot g \cdot \max(z - z_i, 0) - P_i \tag{21}$$

where k is the inlet/outlet pressure loss coefficient, P_{atm} the atmospheric pressure, g the gravity constant, P_i the fluid pressure just beyond the orifice, and z_i the orifice altitude with i the subscript indicating the orifice "from feeding valve" $(in, 1)$, "from tube 6" $(in, 2)$ or "to tube 8" (out).

Finally the water temperature $T = T(P_m, h)$ inside the tank is obtained from the water property tables where $P_m = P_{atm} + \rho \cdot g \cdot \frac{z}{2}$.

Bond graph model

The bond graph representation Figure 12 makes explicit that the feeding tank component exhibits a two-port energy storage (ℂ element) and three multiport energy dissipations (𝕀R elements) connected respectively to the feeding valve, tube 6 and tube 8 components. The energy storage is associated to the state of the water inside the tank. The corresponding energy variables are of generalized displacement type, the mass m and the specific enthalpy h of water. The incompressibility assumption and the integral equations for the water volume give the following relationships [23]:

$$\begin{cases} \rho \cdot A \cdot \dfrac{\mathrm{d}z}{\mathrm{d}t} = \dot{m} \\ \rho \cdot A \cdot z \cdot \dfrac{\mathrm{d}h}{\mathrm{d}t} + h \cdot \dot{m} = \dot{H} \end{cases} \tag{22}$$

where H is the water enthalpy in the tank.

The energy storage behavior laws give the relationships between the energy variables and the conjugated power variables:

$$\begin{cases} P = P_{atm} + \rho \cdot g \cdot z \\ T = T(P_m, h) \end{cases} \quad \text{with } P_m = P_{atm} + \rho \cdot g \cdot \frac{z}{2} \tag{23}$$

The 0-junctions are associated to the conservation laws of the water volume that ideally furnishes $\dot{m}$ and $\dot{H}$ respectively to the energy storage phenomenon if the latter is in integral causality:

$$\begin{cases} \dot{m} = \sum_{i=1}^{2} q_{in,i} - q_{out} & \text{mass conservation (left-hand side 0-junction)} \\ \dot{H} = \sum_{i=1}^{2} q_{in,i} \cdot h_{in,i} - q_{out} \cdot h_{out} & \text{energy conservation (right-hand side 0-junction)} \end{cases} \tag{24}$$

In integral causality the energy storage behavior laws furnish the pressure P and the temperature T to the dissipation phenomena through the 0-junctions. The dissipation phenomena are associated with the singular pressure drops through the inlet and outlet orifices. Each of their corresponding behavior laws is associated to the following equation:

$$k \cdot \frac{q_i \cdot |q_i|}{2\rho} = \max\left(P - \rho \cdot g \cdot z_i, P_{atm}\right) - P_i \qquad \forall i \in \{in1; in2; out\} \tag{25}$$

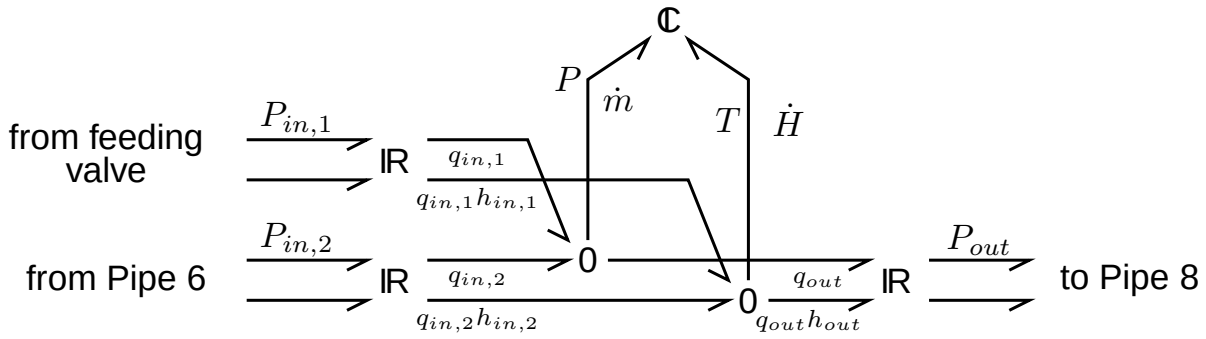

Figure 12: Bond graph representation of the feeding tank

Analysis

Like for the heat exchangers the characteristics of the storage phenomenon says that there are two state variables both of generalized displacement type. In integral causality they are determined by integrating their time derivatives which are given principally by the conservation laws. In return the behavior laws of the energy storage enable to calculate the conjugated variables. The physics of this component [23] says that mass m and enthalpy H of the water in the feeding tank can be taken as state variables and that the corresponding conjugated variables are respectively the pressure P and the temperature T.

Concerning the energy dissipation phenomena, they furnish the different mass flow rates q_i and specific enthalpy flow rates $q_i h_i$ to the conservation laws. In return, they receive the pressure and

the temperature in the feeding tank. Depending on the components connected at their "external" ports and the information received through these ports, the dissipation phenomena will either determine the temperature or the specific enthalpy flow rate for each thermal port (lower bonds), and either the pressure or the mass flow rate for each fluid mechanics port (upper bonds). This physical structural analysis is clearly displayed by the Figure 13 partial causal bond graph. The causal strokes indicates which variables (effort- or flow-like) are furnished by which phenomena. The absence of strokes at the external ports shows the previously mentioned indetermination at this local analysis level. One important consequence will be the type of water property tables that will be required for the dissipation behavior laws.

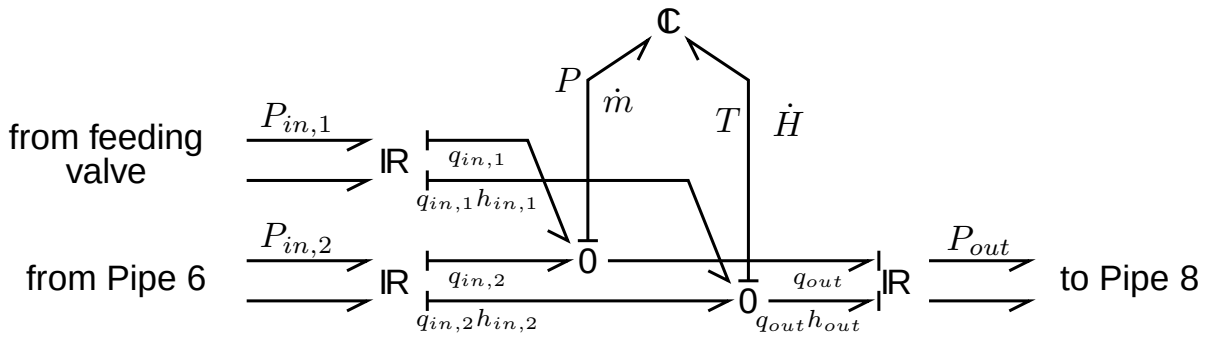

Figure 13: Partial causal bond graph representation of the feeding tank

3.1.3. Centrigugal pump

Modelica model

The pumps ensure the water circulation in the SRI circuit. The model presented here is a dynamic pump model, that integrates the rotating masses equation. This model has two states: the specific enthalpy h of water in the volume of the pump and the angular velocity ω of the pump. The pump is rotated by an electric drive via a mechanical coupler. The iconic diagram in the ThermoSysPro Dymola libray is presented Figure 14.

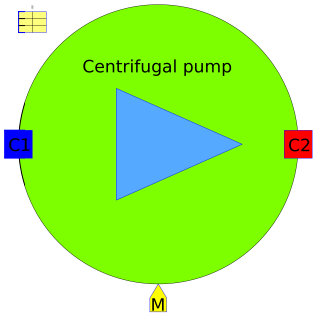

Figure 14: Centrifugal pump block model in ThermoSysPro library of Dymola

The angular velocity ω is governed by the fundamental law of dynamics for rotational mechanics:

$$J \cdot \frac{\mathrm{d}\omega}{\mathrm{d}t} = C_m - C_h - C_f \tag{26}$$

where J is the total rotor inertia, C_m the electric drive torque, $C_h = C_h(\omega, q)$ the resistant hydraulic torque applied by the fluid on the shaft with q the water mass flow rate through the pump, and $C_f = C_f(\omega)$ the mechanical friction torque on the shaft. Details of the torque expressions are given in Appendix A.2.2.

The energy conservation law for the pump is written:

$$\rho \cdot V \cdot \frac{\mathrm{d}h}{\mathrm{d}t} = -q \cdot \Delta h + C_h \cdot \omega + C_f \cdot \omega \tag{27}$$

where ρ is the water density supposed here constant, V the volume of the pump, and Δh the variation of water specific enthalpy through the pump.

The pressure difference $\Delta P = P_i - P_o$ between the inlet and outlet of the pump is given by the incompressible fluid statics equation:

$$\Delta p = \rho \cdot g \cdot h_n \tag{28}$$

where g is the gravity constant, and $h_n = h_n(\omega, q)$ is the pump head detailed in Appendix A.2.2.

The parameters of the centrifugal pump are given in Table 4 of Appendix A.1.

Bond graph model

The bond graph representation of the pump is given Figure 15. The energy storage phenomenon is reduced to a one-port C-element since the pump volume V is constant so as it is supposed for the water density ρ in this component. Consequently it can be established the relationship between the time derivatives of the specific enthalpy h and the enthalpy H:

$$\rho \cdot V \cdot \frac{\mathrm{d}h}{\mathrm{d}t} = \dot{H} \tag{29}$$

In return the energy storage phenomenon furnishes the temperature T that can be obtained by the water property tables $T(h)$ at the given density ρ.

The unique 0-junction corresponds to the energy conservation law expressed by:

$$\dot{H} = q_i \cdot h_i - q_o \cdot h_o + \delta\dot{Q}_h + \delta\dot{Q}_f \tag{30}$$

where $\delta\dot{Q}_h = C_h \cdot \omega$ is the heat flow rate due the hydraulic resistance and $\delta\dot{Q}_f = C_f \cdot \omega$ the heat flow rate due to the mechanical friction on the pump shaft. These terms are furnished by a two- and a one-port dissipation phenomenon respectively (R-elements), which occur in the rotational dynamics of the pump. This rotational dynamics is represented by a conservation law (Equation (26)) associated to a 1-junction that collects the terms from the energy storage (I-element), the energy source (Se-element) and the dissipation phenomena (R-elements). The behavior laws of the dissipation phenomena expressed the resistive torques on the shaft given in Appendix A.2.2.

Finally the pressure drop ΔP is related to the inlet et outlet pump pressures through the 1-junction to which is associated the mass flow rate q. The dissipation phenomenon gives the last relationship between this pressure drop and both the pump shaft angular velocity ω and the mass flow rate (by the intermediary of the pump head h_n expressed by Equation (47)).

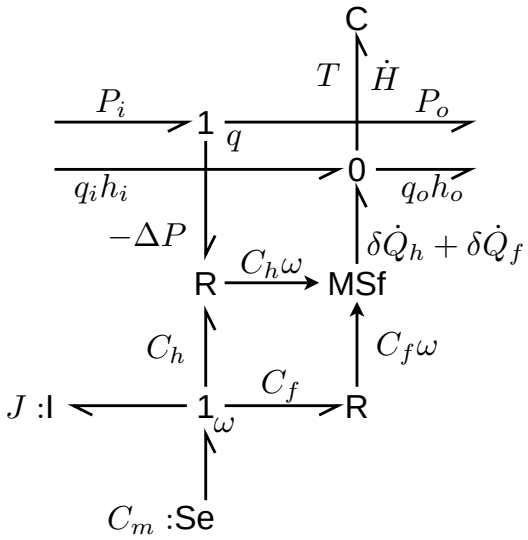

Figure 15: Bond graph representation of a pump

Analysis

The preferred integral causality for the energy storage phenomenon leads to the partial causal assignment of the pump bond graph (Figure 16). This shows that the time derivative of the water enthalpy is furnished to the energy storage phenomenon by the energy conservation law. The energy storage phenomenon returns back the temperature that is transmitted to the pump inlet and outlet.

Concerning the fluid domain, in particular involving the dissipation phenomena, different variable assignments may happen depending on the environmental components connected at the corresponding ports. If the mass flow rate is determined by the connected component at one of the pump fluid ports (either inlet or outlet), one pressure by the one at the other pump fluid port, then the pressure drop is calculated by the dissipation behavior phenomenon which determines the pressure at the first pump fluid port. A second possibility is that both pressures at the pump fluid external ports are imposed by the corresponding connected components. These pressures determine the pressure drop that in turn is used by the dissipation behavior law to furnish the mass flow rate to the external components. This organization of the equations is conditioned by the invertibility of the dissipation behavior law. The expression of the pump head (Equation (47)) is probably the main limit to this second variable assignment. This will be subject to discussion in the global phase of physical structural analysis with the connection of the different components.

3.1.4. Valves

Modelica model

Three types of valves are considered in the SRI model: regulation valves at the heat exchanger outlets, the on/off valve for the feeding tank and the users' valve for the auxiliary equipment (Figure 17). All are modeled by singular pressure drops with the same form of dissipation behavior law but with different opening rules. The regulation valves have variable opening depending on the controller law (not modeled here). The users' valve is supposed open at a fixed and maximal

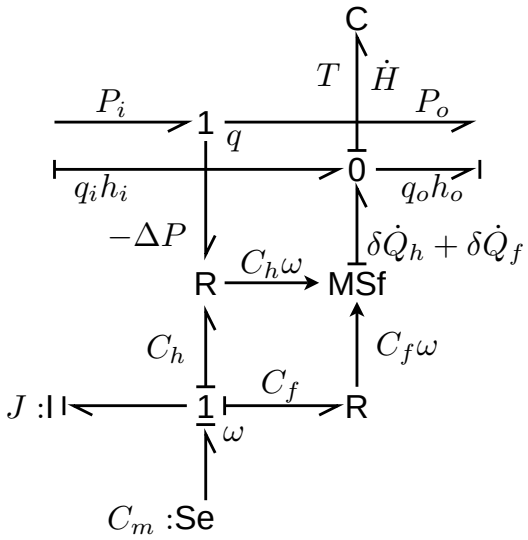

Figure 16: Partial causal bond graph representation of a pump

given value. The feeding valve is either open or closed.

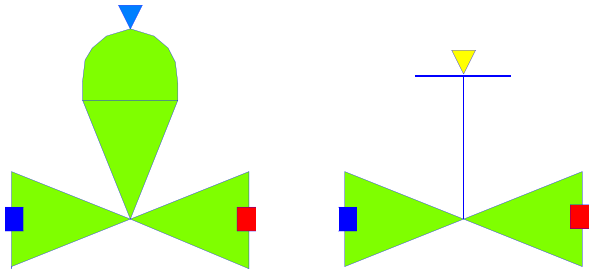

Figure 17: Dymola iconic diagrams for regulation or users', and on/off valves

The pressure drop $\Delta P = P_i - P_o$ verifies the following expressions depending on the valve type:

$$\begin{cases} \text{for the regulation valves} & \Delta P \cdot [Ouv(t) \cdot C_v^{max}]^2 = \frac{1.733 \cdot 10^{12}}{\rho^2} \cdot q^2 \\ \text{for the users' valves} & \Delta P \cdot (C_v^{max})^2 = \frac{1.733 \cdot 10^{12}}{\rho^2} \cdot q^2 \\ \text{for the feeding on/off valve} & \begin{cases} \Delta P = \frac{k}{2\rho} \cdot q^2 & \text{valve on} \\ q = q_{min} & \text{valve off} \end{cases} \end{cases} \tag{31}$$

where P_i and P_o are the pressures at the inlet and outlet respectively, $Ouv(t)$ an opening time function imposed by the controller, C_v^{max} a characteristic parameter of the valve, ρ the water density supposed here constant, q the masse flow rate through the valve, k the singular pressure drop coefficient, and q_{min} the minimal mass flow rate when the feeding valve is off.

The water temperature is determined from the water property tables:

$$T_m = T_m\left(P_m, h_m\right) \tag{32}$$

with averaged values of the pressure and the specific enthalpy given by:

$$\begin{cases} P_m = \dfrac{P_i + P_o}{2} \\ h_m = \dfrac{h_i + h_o}{2} \end{cases} \tag{33}$$

where h_i and h_o are the water specific enthalpies at the valve inlet and outlet respectively.

The parameters of the valves are given Table 5 in Appendix A.1.

Bond graph model

The bond graph representation is similar to the one used for dissipation effects at the boundary between two control volume in the heat exchanger (see Section 2) or through orifices of the feeding tank (see Section 3.1.2) since it corresponds to singular pressure drops (Figure 18). It also exhibits a modulation that is the opening law $Ouv(t)$ for the regulation valves, not activated for the users' valve and an on/off signal for the feeding tank.

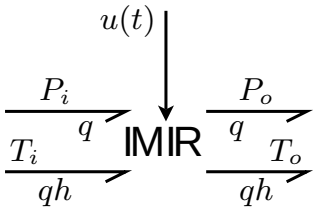

Figure 18: Bond graph representation for the dissipation effects through a valve

The behavior laws attached to these dissipation phenomena are given by Equations (31) which can be conveniently rewritten into the following forms depending on the variables imposed by the environmental components at the external ports of this phenomena:

$$\begin{cases} \text{for the regulation valves} & q = Ouv(t) \cdot C_v^{max} \cdot \frac{\rho}{\sqrt{1.733 \cdot 10^{12}}} \cdot \sqrt{|\Delta P|} \cdot \operatorname{sgn} \Delta P \\ \text{for the users' valves} & q = C_v^{max} \cdot \frac{\rho}{\sqrt{1.733 \cdot 10^{12}}} \cdot \sqrt{|\Delta P|} \cdot \operatorname{sgn} \Delta P \\ \text{for the feeding on/off valve} & \begin{cases} q = \sqrt{\frac{2\rho}{k} \cdot |\Delta P|} \cdot \operatorname{sgn} \Delta P & \text{valve on} \\ q = q_{min} & \text{valve off} \end{cases} \end{cases} \tag{34}$$

Analysis

The models of valves presented do not exhibit any storage phenomenon. They have static behaviors. This confers flexibility for assigning the different variables depending on the causality of environmental components that they may impose. Nevertheless it is conditioned by the possibility of inverting the dissipation behavior law i.e. the possibility of equally using Equations (31) or (34). Another consequence is once again the water property tables required. For instance the second form of behavior laws (Equations (34)) requires the specific enthalpy $h = h(P_m, T_m)$ where averaged pressure $P_m = \frac{P_i+P_o}{2}$ and temperature $T_m = \frac{T_i+T_o}{2}$ can be taken. The final choice is done at the global level of the physical structural analysis.

3.1.5. Lumped straight pipes (circular duct)

Modelica model

The dymola sketch of a straight pipe model is presented Figure 19. Every phenomenon continuously distributed all along the pipe is considered localized at one point for approximation.

Figure 19: Pipe block in ThermoSysPro library of Dymola

In this model no change of mass flow rate neither the specific enthalpy flow rate is supposed between the inlet and outlet of the pipe. This states:

$$\begin{cases} q_i = q_o \\ h_i = h_o \end{cases} \tag{35}$$

where the subscripts i and o stand for inlet and outlet respectively.

The application of the momentum conservation law on the pipe gives the total pipe pressure drop $\Delta P = P_i - P_o$:

$$\Delta P = \begin{cases} \Delta P_f + \rho \cdot g \cdot \Delta z + \frac{L}{A} \cdot \frac{\mathrm{d}q}{\mathrm{d}t} & \text{with inertia effect} \\ \Delta P_f + \rho \cdot g \cdot \Delta z & \text{without inertia effect} \end{cases} \tag{36}$$

where ρ is the water density supposed here constant, g the gravity constant, Δz the inlet/outlet altitude change, L the pipe length, and A the duct cross-sectional area.

ΔP_f corresponds to the pressure loss due to friction in the pipe. It is expressed by:

$$\Delta P_f = \frac{k}{2 \cdot \rho} \cdot q^2 \operatorname{sgn} q \tag{37}$$

where k is the regular pressure drop coefficient.

Finally the water property tables furnish an averaged temperature in the pipe:

$$T_m = T_m \left(P_m, h_i \right) \tag{38}$$

where the average pressure is given by:

$$P_m = \frac{P_i + P_o}{2} \tag{39}$$

The parameters of pipes are given Table 6 in Appendix A.1.

Bond graph model

The bond graph representation of a pipe model is presented in Figure 20. It shows an energy storage (I-element) for the inertia effects along the pipe. If they are not taken into account, this element simply vanishes. The pressure drop due to the gravity effect is represented by an effort source and the one due to friction by an R-element.

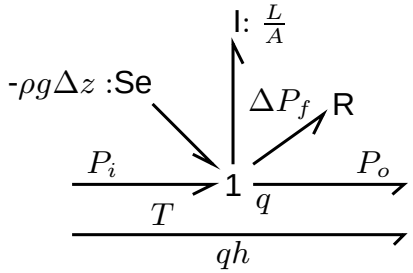

Figure 20: Bond graph representation of pipe models

The behavior law associated to the energy storage is linear and states that the fluid momentum is proportional to the mass flow rate where $\frac{L}{A}$ is the coefficient. The behavior law associated to the dissipation effects for friction is given by Equation (37). The bond graph representation proposed for this model consider continuity of mass flow rate, specific enthalpy flow rate and also temperature. If one wishes a temperature gradient to be modeled along the pipe, second port on the dissipation phenomenon can be added and connected to a 1-junction inserted on the thermal domain. In that case this requires the use of water property tables, in particular, to define the water specific enthalpy.

Analysis

The key issue of the physical structure analysis at this component level is the assumption about the inertia effects. If they are considered and that integral causality is preferred, then the energy storage receives the balance of effort-like variables (the pressures at the pipe inlet and outlet, the pressure loss due to friction and the one due to gravity effect to compute the mass flow rate imposed to the pressure drops behavior laws and to the pipe external ports. On the contrary if no inertia effect is supposed then one external connected component has to furnish one pressure and the other one the mass flow rate. The final decision is to be made at the global level of the physical structure analysis.

Furthermore the thermal domain representation (lower bond of Figure 21 bond graph) states the continuity of both specific enthalpy flow rate and temperature. If the former is imposed at one external port the temperature cannot be also imposed at the same port. Now if a temperature gradient along the pipe is supposed still with the continuity of specific enthalpy flow rate this may enable to impose both temperatures from the external connected component (Figure 22). In that case specific enthalpy can be obtained from water property tables in termes of an averaged temperature and the water density: $h = h(\frac{T_i+T_o}{2}, \rho)$.

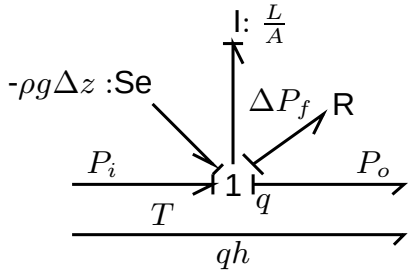

Figure 21: Partial causal bond graph of a pipe

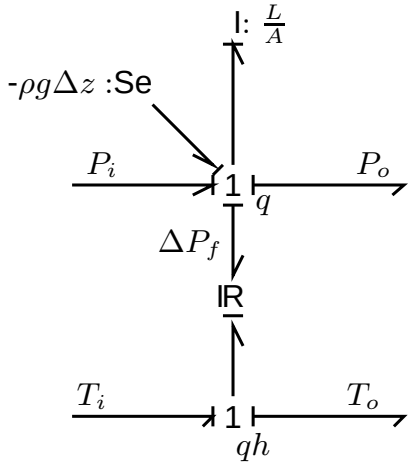

Figure 22: Causal bond graph of a pipe with temperature gradient

3.1.6. Circuit junctions

Modelica model

The last component to inspect in the SRI model is a junction of several pipes at some node of the circuit. The Modelica model proposes to consider a volume with energy storage effects. This is equivalent to modeling a control volume as presented for the heat exchanger (Equations (1) and (5)) but with no heat exchange. These equations state the mass flow rate and the energy conservation for the control volume (see Section 2). One may also consider static mass balance in which case the mass conservation law simply becomes a net balance or input and output mass flow rates.

Bond graph model

According to the analogy above the bond graph model of a volume for a circuit junction is the same as the Figure 7 with the corresponding equations (see Section Section 2) but without the bond associated to the heat exchange and as many pairs of thermofluid bonds as the number of merging pipes. If one wishes to idealize the circuit junction neglecting the volume storage effect one simply takes off the C-element leaving only bonds and 0-junctions.

Analysis

Due to the analogy the physical structural analysis is similar. The preferred integral causality for the energy storage imposes the effort variables to the environmental connected components: the pressures for the fluid domain and the temperatures for the thermal domain. Figure 23 shows the causal bond graph for a junction with energy storage phenomena in preferred integral causality and three connecting pipes one inlet and two outlets. This feature will be advantageously used at the global level when connecting these junction models to the pipe ones.

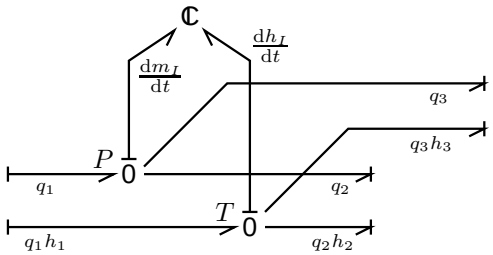

Figure 23: Causal bond graph of a junction with energy storage phenomena

The flexibility of neglecting the energy storage phenomena shall also enable to match particular causality requirements from certain connected components. For instance an idealized version of a junction with no energy storage phenomenon is shown Figure 24. In that case one pair and only one pair of pressure and temperature variables will be imposed by an external connected component (here on port 1). It is not necessary that these effort variables be on the same inlet or outlet. The only constraint is that one pair and only one must be imposed from outside the junction component.

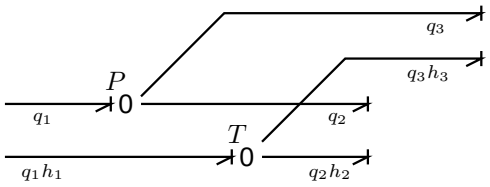

Figure 24: Causal bond graph of an idealized junction component

3.2. Global phase: system level

3.2.1. Bond graph model

The word bond graph for the whole SRI is built by connection of the different component bond graph representations identically to Figure 2 sketch. All connections are constituted of two ports for the fluid and the thermal domains respectively (Figure 25). The boundary conditions have been added by means of effort sources for the imposed pressures and temperatures. Since the leak has been neglected in the auxiliary equipment, the boundary condition BC6 only refers to the pressure. At this location and on the thermal bond, a flow source figures the source of heat. Finally

the controlled temperature at outlet of the cooling systems is materialized in the bond graph by an effort detector placed on the thermal corresponding bond.

For the reading commodity of the bond graph representation the convention to place the fluid bonds on top or on the left-hand side has been adopted.

The different "words" refers to the following bond graph representations:

heat exchangers: figure 6 page 10,

Valves: figure 18 page 22,

Junctions: figure 23 page 26 if volumes are taken into account and figure 24 page 26 they are idealized,

Pipes: figure 21 page 25 or figure 22 page 25 depending on the causality requirements,

Tank: figure 13 page 18,

Pumps: figure 16 page 21.

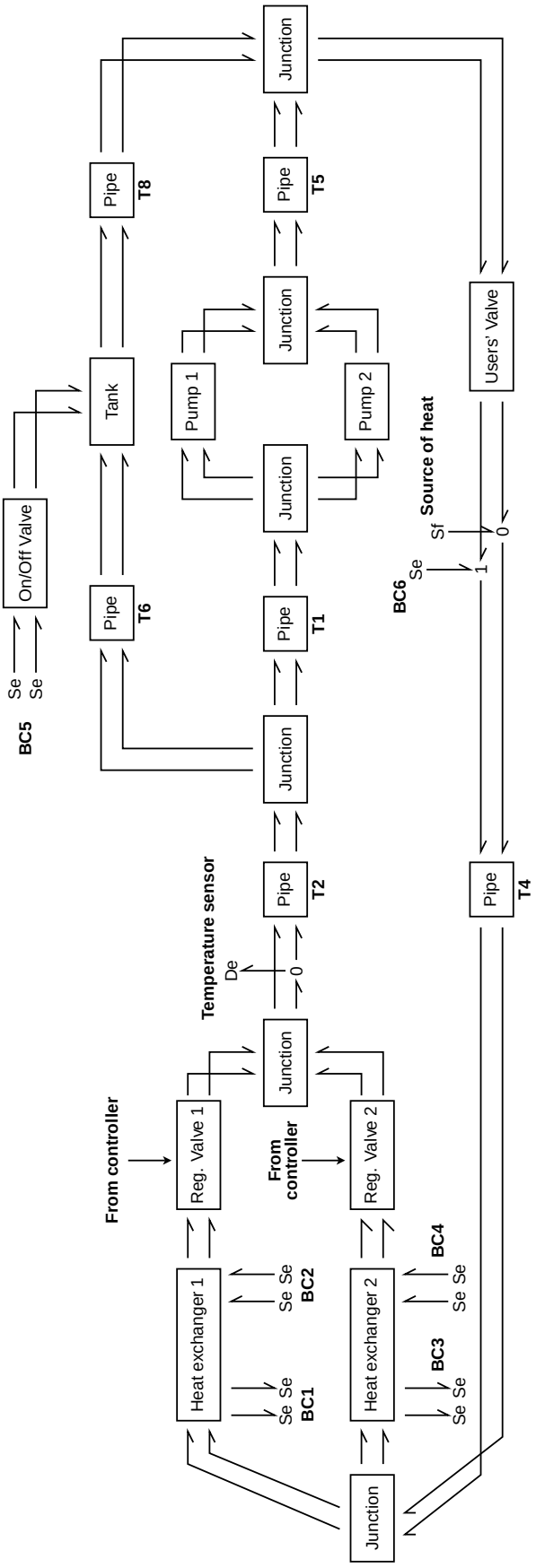

Figure 25: Word bond graph of SRI

3.2.2. Analysis

The first step in the physical structure analysis at the global level is to ensure the causal consistency in the connection of the different component models. The analyses undertaken at the local level helps for this task.

Starting with the exchangers the preferred integral causality on the energy storage phenomena leads to completely assign the model. Their external port causality for the cold branches (both pressures and temperatures should be received by the exchangers) is consistent with the boundary conditions that impose both the effort variables. For the hot branches the consequence is that the adjacent components (a junction upstream and the regulation valves downstream) have to impose the effort variables as well. This is the case with the junction modeled with energy storage effects (volume). Concerning the valves this requires that pressure and temperature be imposed on the outlet ports (Figure 26) and the use of Equations (31) form to calculate the pressure drop and then the pressure at the inlet port, the mass flow rate being furnished at the same port by the exchanger component. In the thermal domain the water properties must give the specific enthalpy $h = h(P_o, T_o)$ in terms of the outlet pressure and temperature. In turn the specific enthalpy flow rate can be determined as well as the temperature at the inlet $T_i = T_i(P_i, h)$ in terms of the previously calculated inlet pressure and the specific enthalpy.

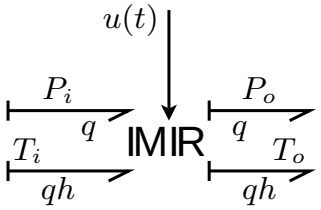

Figure 26: Causal bond graph representation for the regulation valves

Downstream the regulation valves the junction component has to furnish both effort variables (pressure and temperature) which is consistent with the model including volume storage effects. In cascade this propagates the effort assignment to the pipe T2. Now if the junction component has volume storage phenomena, both pressure and temperature at the inlet of the pipe T2 component. This leads using the figure 22 which admits a temperature difference between inlet and outlet. Then the pressure and temperature assignments can be propagated until the pipe T1 and T6 components.

At this stage it is worth to address the circulation system constituted of the two pumps. The preferred integral causality requirements leads to causal conflicts on the 0-junctions associated to the energy conservation laws in the junction components (Figure 27). It is even worse noting that the above mentioned 0-junctions are finally directly connected making statically dependent to each other the energy storage phenomena in the four components for the thermal domain [3].

The solution to circumvent this problem that would let the model compiler to reduce the resulting DAE index might be not satisfying. The physical structure analysis of this part of the system

[3] It is worthwhile to note that neglecting the volume storage effects in the junction components does not solve the problem still leaving a causal conflict on the 0-junctions corresponding to a direct statically dependence between the pump energy storages.

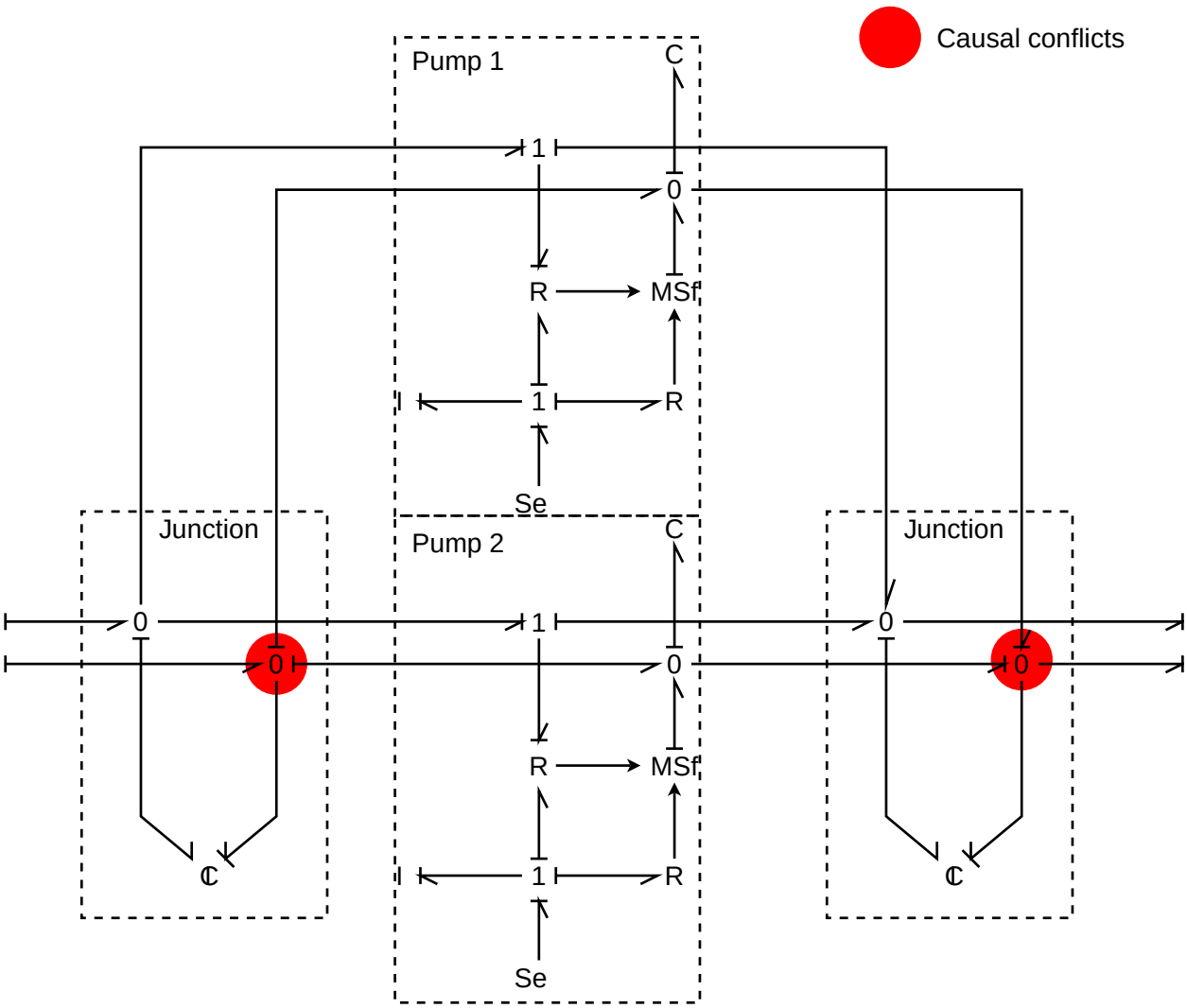

Figure 27: Causal conflicts in the bond graph of the circulation system

indicates that phenomena introduced between the involved components can solve the above mentioned problem. In particular inserting multiport dissipation phenomena can eliminate the conflict and guaranty the preferred integral causality for every energy storage phenomenon. The resulting bond graph representation is given Figure 28 with multiport R-elements. They can be physically interpreted as regular pressure drop already encountered for the pipe component (Figure 22) where inertia and gravity effects are neglected.

The rest of the model can be assigned without any difficulty taking into account of inertia effect and temperature difference in every pipe, and volume storage phenomena in every junction (figure 29). The preferred integral causality is respected for every energy storage. The number of their ports indicates the number of independent state variables for the whole model and thus, the number of initial conditions needed and on which physical varables they are defined. The heat exchangers have 20 such variables (masses and specific enthalpies in each control volume), the junctions: 2 each (mass and specific enthalpy), the pipes: 1 each (fluid momentum), the pumps: 2 each (water specific enthalpy in the volume and angular momentum of shaft) and the tank: 2 (water mass or height and specific enthalpy in the volume). The total is thus 64 independent state

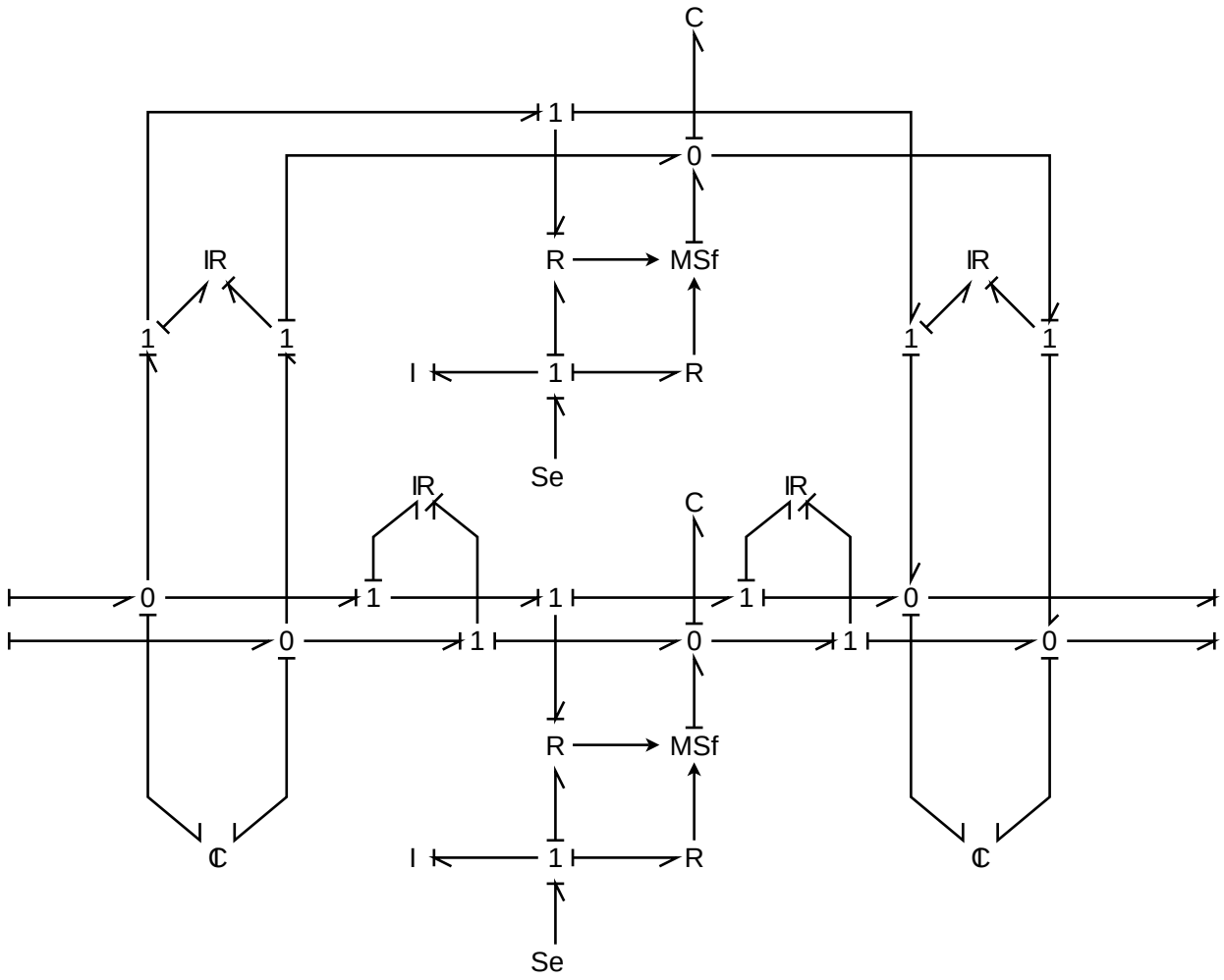

Figure 28: Causal bond graph of the circulation system without conflict

variables for this model.

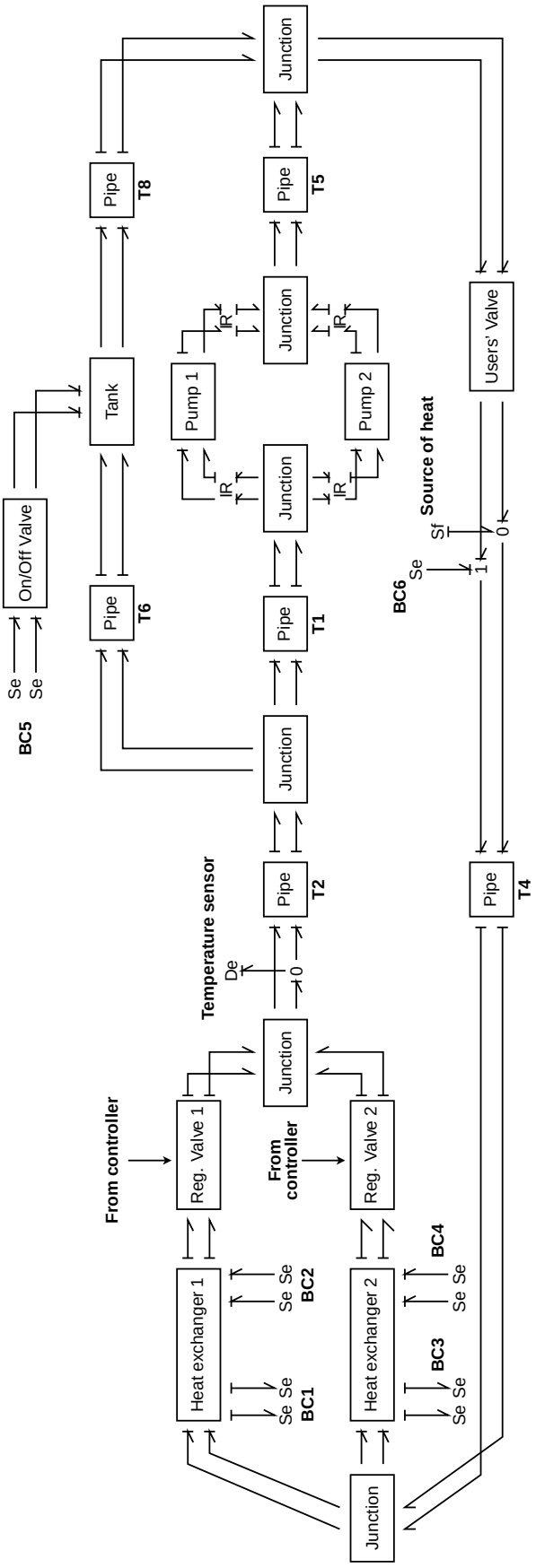

Figure 29: Causal word bond graph of SRI

4. State estimation

4.1. Problem position

The state estimation of an exchanger is used in order to illustrate one of the benefits of the physical structural analysis. It must be emphasized that the method adopted is based on model inversion. From the Bond Graph model analysis, twenty state variables are defined, two for each of the five lump port storage phenomena in the hot and the cold branches. These storage ports are all in integral causality which means that they are statically independent. If no particular functioning conditions are prescribed twenty informations are required to fix the initial conditions of all these states.

However from outside, the exchanger it can be seen that only four power lines can attain the inside[4], so potentially four state variables are susceptible to be determined from outside measurements (Figure 30) while, depending on which state variables are estimated, until sixteen could be fixed. Now the question to be raised is: can any combination of four state variables be simultaneously determined? The physical structural analysis helps know which combinations are valid.

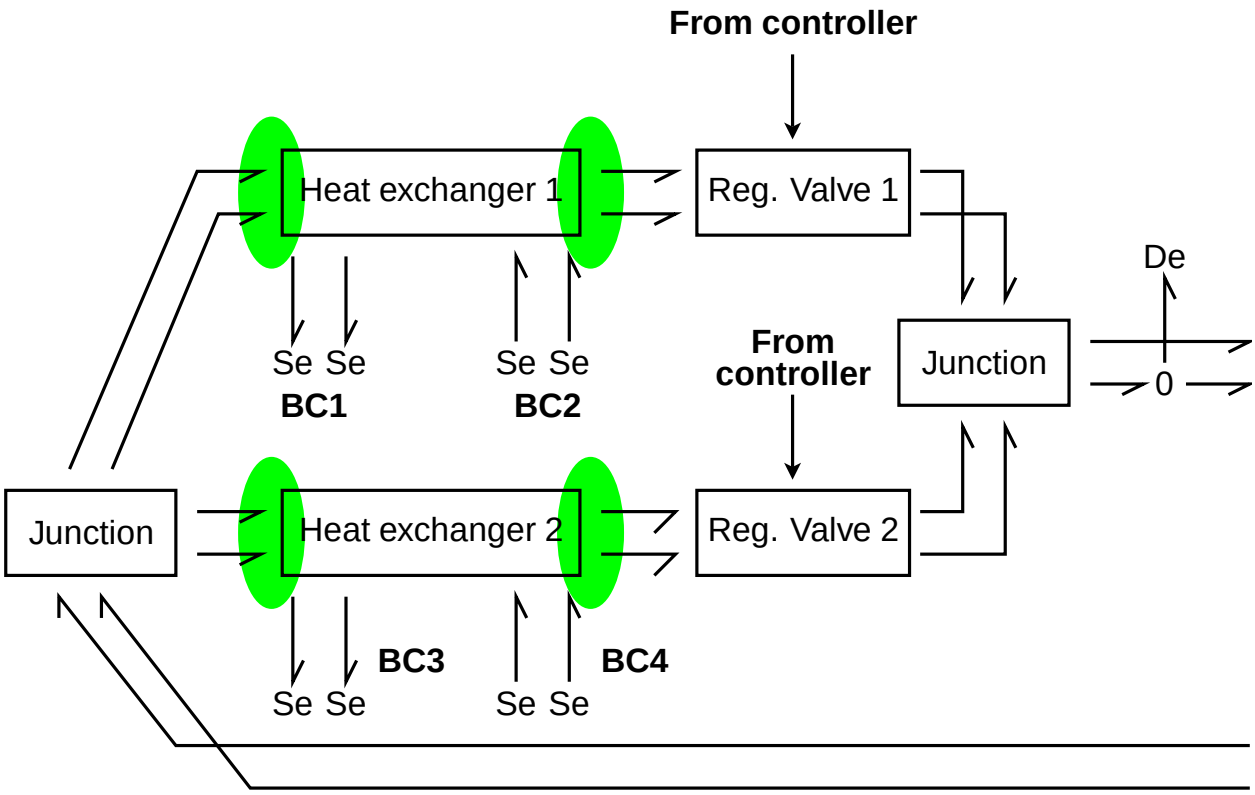

Figure 30: Visualization of the four external ports of an exchanger

A last important remark concerns the measurements that, due to the nature of the external ports of the exchanger, must be done on only one conjugated power (pseudo-)variables per port. An illustrative (and intuitive) choice is the two pressures and two temperatures at both the inlet and outlet of the exchanger.

[4]It is supposed that no measurement are undertaken on the cold water circuit.

4.2. Acausal criterion

The first criterion requires the existence of a set of disjoint power lines [5] between the state variables targeted inside and the potential nodes of measurement outside the exchanger. A detailed investigation of the exchanger bond graph shows that a combination of four disjoint power lines starting from any set of four storage ports inside the exchanger and reaching the four external ports of the exchanger is possible. This criterion is acausal and only necessitates to inspect the series of power bonds on the bond graph i.e. the series of powers and the relationships between these powers in the model. This criterion is included in the next one but the interest of applying it first lies in the fact that if it is not verified, the problem of state estimation has to be restated without need to go further in the analysis (Figure 31).

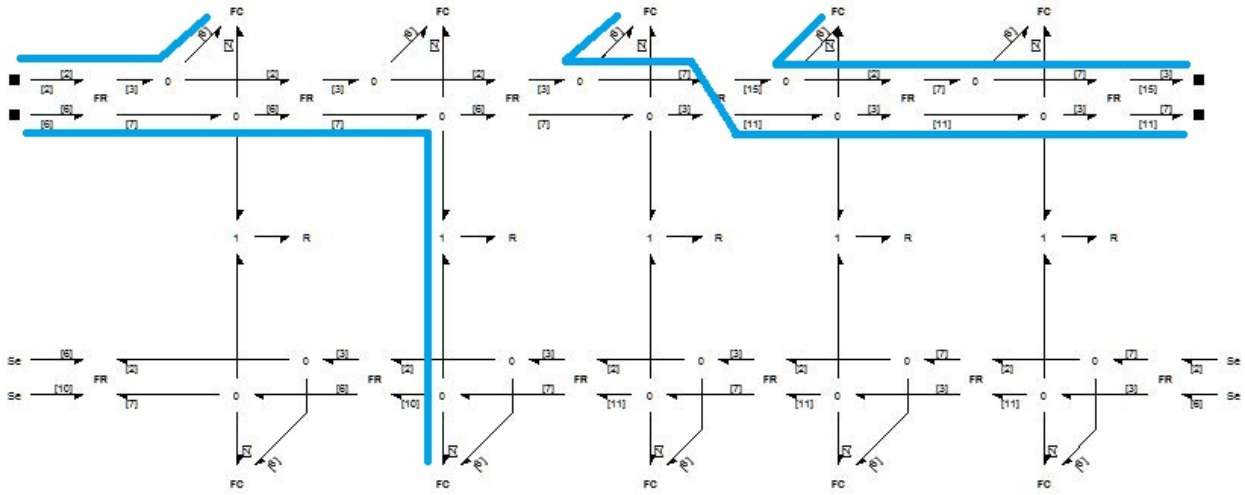

Figure 31: Example of a combination of four disjoint power lines

4.3. Causal criterion

Then the second criterion inspects the existence of a set of disjoint causal paths between the storage ports and the external ports of the exchanger. It goes a step further by verifying the structural existence of possible disjoint relationships that will be potentially invertible to undertake the desired state estimation. Once again this is a necessary but not a sufficient condition. This is required and if the criterion is not verified, then no attempt to pursue the state estimation by model inversion is necessary. The inspection of the causal bond graph shows that there exists a combination of four disjoint causal paths from any storage ports to the external ports of the exchanger.

At this point further information can be stated from the order concept of a causal path. From the causal bond graph representation it can be seen that the further inside the exchanger is the starting storage port, the greater is the order of the corresponding causal path. It is due to the fact that in this case the causal path encounters one or several storages in integral causality. The consequence is that in the exploitation of the inverse model, not only the measurement signals will be needed but also their time derivatives at least until the order indicated by the causal path. Of course, the functioning conditions in which measurements are done can circumvent these difficulties like steady state behaviors for instance which set to zero the state time derivatives.

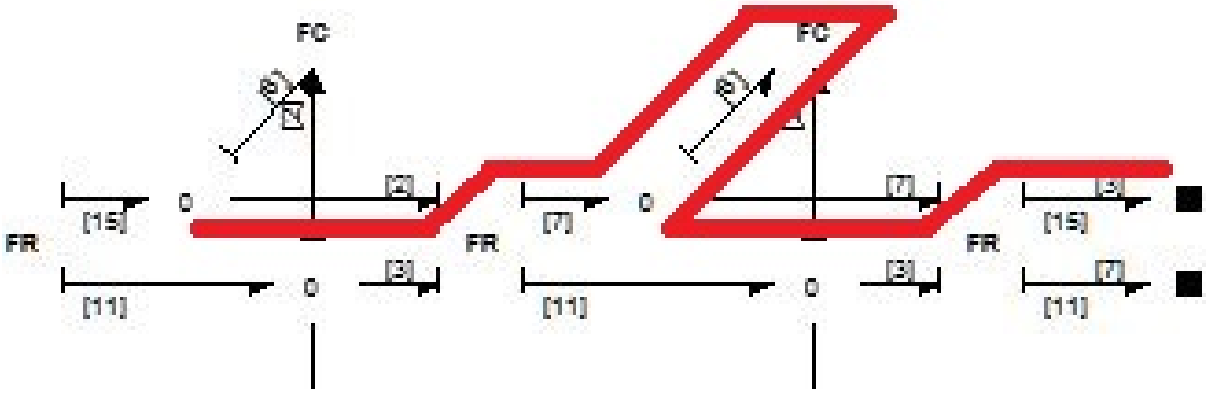

Figure 32: Example of a causal path of order 1

Here once again no simulation has been needed for the physical structural analysis.

4.4. Model inversion

The next and final step is to organize the model equations in order to determine the state variables that have to be estimated in terms of the variables at the external ports of the exchanger. At this stage, a careful inspection of the dissipation phenomena shows the appearance of algebraic loops that have to be solved inside the dissipation phenomena.
Far from being exhaustive this analysis has concentrated on the exchanger and must be viewed only as an illustration of what physical structural analysis can bring to some model-based engineering objectives. However it can be reproduced anywhere in the rest of the model. It depends on the possible measurement nodes and the state variables that one wants to estimate. Moreover the analysis can also be applied for input reconstruction, control input synthesis and to some extent can help for parameter identification, each of these activities being based on model inversion.

5. Modelica language specifications

Modelica language specifications for undertaking physical structural analysis is essentially a question to annotate the variables and the equations in order to keep a trace of the different concepts presented in [5]. The information annotated may be redundant with what the language can already give but this redundancy may be exclusively dedicated to the physical structural analysis.

Informations that must be underlined are:

- on the nature of variables:
  - power variables (effort, flow or pseudo-),
  - energy variables (generalized displacement and generalized momentum),
  - intermediary variables (other than the above ones).
- on the role of variables:
  - state variables,

  - input and output variables,
  - modulation variables.
- on the nature of relationships:
  - behavior laws,
  - conservation laws of physics,
  - calculus relations (other than the above ones).
- on the physics fundamental concepts:
  - elementary physical phenomenon (storage, dissipation, source, sink),
  - multiport phenomena,
  - energy transduction.

The physical structural analysis concepts to define in Modelica language:

- power lines (simple, of energy supply, of modulation, input/ouput),
- storage phenomenon in integral/derivative causality,
- causal paths (input/output).

Analysis concepts that the Modelica language must be able to determine:

- a set of joint/disjoint power lines,
- a causality assignment not necessarely accompanied with a simulation model compiling,
- a set of joint/disjoint causal paths,
- the order of a causal path and of a set of causal paths,
- the output essential order.

Elements of procedure that the Modelica language must permit:

- definition of the variables of interest for the analysis,
- search of the analysis concepts (power lines, causal paths, set of power lines, set of causal paths,
- test of the analysis criteria (acausal, causal, output differentiability),
- derivation of the inverse model.

6. Conclusion and perspectives

Unfortunately some events during the project have prevented from the complete study of the ECS use-case. This is the reason why it was decided to present nothing on it in this report even if a bond graph structure was set during an end-of-studies project of a student in laboratory Ampère. Only the SRI system has been thoroughly studied but the methodology and the main issues of analyses can be reproduced for the ECS.

This report has presented the application of the physical structure analysis on the SRI use-case. Two main phases are proposed: at the local level on the different components of the system and at the global level for the whole system. It has been shown how the local level of analysis brings valuable information to address issues at the global level. It must be emphasized that these analyses are undertaken before any numerical simulation or even the model compilation. However the analyses furnish important results that help to tackle potential problems in the modeling phase, to anticipate simulation difficulties, to guide on how to correctly set an engineering problem, and the most importantly, to link every analysis result to the physics of the system.

The main results of analysis have been presented in the context of the bond graph representation. It intrinsically carries the physical and analysis concepts required for the physical structure analysis presented. Though the Modelica language shares common features with the bond graph formalism like the acausal feature, it lacks of the concepts required for this type of analysis. Thus Modelica language specifications have been proposed from the SRI study to fill the gap.

The perspectives are to complete the studies in particular for the ECS and to develop the Modelica language extension to introduce the concepts of physical structural analysis on the specifications basis given in this report and in [5]. Finally it can be noticed that graphical description of a model helps conduct physical structural analyses and bond graph is a good example for this. Iconic description is not sufficient and it would be interesting to develop graphic annotations in the Modelica language that exhibit the concepts of physical structural analysis.

References

[1] D. Bouskela. Modrio full project proposal. Technical Report version 2.3, ITEA2, Feb. 06, 2015.

[2] E. Thomas and E. Ledinot. Requirements for static model analysis. MODRIO deliverable D6.1.1 version 0.5, Dassault-Aviation, 2013.

[3] A. Jardin and Thoma E. Intermediate and final report static model analysis. Modrio deliverable d6.1.2, Dassault-Aviation, EDF, 2014.

[4] Furic S. and P. Magnin. Static model analysis module based on bond graph and synchronous approaches. MODRIO deliverable D6.1.3 version 1.0, Siemens LMS-Imagine, 2014.

[5] Marquis-Favre and M-T. W, Pham. D.6.1.4 - methodology and specification report for static model analysis - theoretical concepts and analysis procedure (m33 version). Technical Report version 1.1, Ampère Laboratory - CNRS, 2016.

[6] D.C. Karnopp, Margolis D.L., and R.C. Rosenberg. System dynamics: Modeling, simulation, and control of mechatronic systems, fifth edition. In *John Wiley & Sons, Inc.*, Hoboken, NJ, USA., 2012.

[7] B. El Hefni. Dynamic modeling of concentrated solar power plants with the thermosyspro library (parabolic trough collectors, fresnel reflector and solar-hybrid). In *Energy Procedia*, volume 49, pages 1127–1137, 2014.

[8] Open-modelica: http://build.openmodelica.org.

[9] B. El Hefni and D. Bouskela. Modeling of a water/steam cycle of the combined cycle power plant "rio bravo 2" with modelica. In *Modelica conference proceedings*, 2006.

[10] B. El Hefni, D. Bouskela, and G. Lebreton. Dynamic modelling of a combined cycle power plant with thermosyspro,. In *Proceedings of the 9th International Modelica Conference*, Munich, Germany, September 3-5 2012.

[11] D. Bouskela B. El Hefni and G. Lebreton. Dynamic modelling of a condenser/water heat with thermosyspro. In *Proceedings of the 8th International Modelica Conference*, volume 63, pages 365–375, Linköping, Linköping University Electronic Press, 2011.

[12] O. Deneux, B. El Hafni, B. Péchiné, E. Di Penta, G. Antonucci, and P. Nuccio. Establishment of a model for a combined heat and power plant with thermosyspro library. In *Procedia Computer Science*, volume 19, pages 746–753, 2013.

[13] Dymola 2016 fd01 dynasim ab. lund, sweden: http://www.dymola.com.

[14] Wolfgang Wagner and Hans-Joachim Kretzschmar. *International Steam Tables - Properties of Water and Steam based on the Industrial Formulation IAPWS-IF97*. Springer-Verlag Berlin Heidelberg, 2008.

[15] R. Shoureshi and M. Kevin. Analytical and experimental investigation of flow-reversible heat exchangers using temperature-entropy bond graphs. In *American Control Conference*, pages 1299–1304, 22-24 June 1983.

[16] M. Hubbard and J.W. Brewer. Pseudo bond graphs of circulating fluids with application to solar heating design. In *Journal of the Franklin Institute*, volume 311, pages 339–354, 1981.

[17] M. Delgado and J. Thoma. Bond graph modeling and simulation of a water cooling system for a moulding plastic plant. In *Systems Analysis Modeling Simulation*, volume 36, pages 153–171, 1999.

[18] D.C. Karnopp and S. Azerbaijani. Pseudo bond graphs for generalised compartmental models in engineering and physiology. In *Journal of the Franklin Institute*, volume 312, pages 95–108, 1981.

[19] D.C. Karnopp. Pseudo bond graphs for thermal energy transport. In *Journal of Dynamic Systems, Measurement and Control*, volume 100, pages 165–169, 1978.

[20] D.C. Karnopp. State variables and pseudo-bond graphs for compressible thermo-fluid systems. In *Journal of Dynamic Systems, Measurement and Control*, volume 101, pages 201–204, 1979.

[21] D.C. Karnopp and S. Azerbaijani. Pseudo bond graphs for generalised compartmental models in engineering and physiology. In *Journal of the Franklin Institute*, volume 312, pages 95–108, 1981.

[22] B. Ould Bouamama. Bond graph approach as analysis tool in thermo-fluid model library conception. In *Journal of the Franklin Institute,*, volume 340, pages 1–23, 2003.

[23] F. M. White. *Fluid Mechanics*. McGraw-Hill, seventh edition in si units edition, 2011.

[24] The simulation program MS1: http://www.lorsim.be.

A. Appendix

A.1. Parameters of SRI

Table 1: Boundary conditions

Name	Value	Description
P_{BC1}, P_{BC3}	3	BC1 and BC3 pressures [bar]
T_{BC1}, T_{BC3}	285	BC1 and BC3 temperatures [K]
P_{BC2}, P_{BC4}	1	BC2 and BC4 pressures [bar]
T_{BC2}, T_{BC4}	285	BC2 and BC4 temperatures [K]
P_{BC5}	3	BC5 pressure [bar]
T_{BC5}	290	BC5 temperature [K]
P_{BC6}	1	BC5 pressure [bar]
T_{BC6}	290	BC5 temperature [K]

Table 2: Parameters of heat exchangers

Name	Value	Description
N	5	Number of exchanger segments [-]
$V_{b,I}$	0.25	Volume of control volume [m^3]
$c_{1,h}$	1.12647	Pressure drop correction factor for hot branch [-]
$c_{1,c}$	1	Pressure drop correction factor for cold branch [-]
n	499	Number of plates [-]
S_p	2	Surface of the plate [m^2]
e_m	0.0006	Metal thickness [m]
λ_m	15.0	metal thermal conductivity [W/(m.K)]

Table 3: Parameters of the feeding tank

Name	Value	Description
ρ	998	Water density in the tank [kg/m^3]
A	7	Tank cross sectional area [m^2]
k	1	Inlet/outlet pressure loss coefficient [-]
P_{atm}	1.013e5	atmospheric pressure [Pa]
g	9.80665	Gravity constant [m/s^2]
$z_{in,1}$	40	Altitude of inlet 1 [m]
$z_{in,2}$	0	Altitude of inlet 2 [m]
z_{out}	0	Altitude of outlet 1 [m]

Table 4: Parameters of pumps

Name	Value	Description
J	10	Moment of inertia [kg.m^2]
ρ	998	Water density in the pump volume [kg/m^3]
V	1	Pump volume [m^3]
g	9.80665	Gravity constant [m/s^2]
b_1	-3.7751	Characteristic coefficient of pump hydraulic efficiency [m^{-6}s^2]
b_2	3.61	Characteristic coefficient of pump hydraulic efficiency [m^{-3}s]
b_3	-0.0075464	Characteristic coefficient of pump hydraulic efficiency [-]
N_{nom}	1400	Nominal angular velocity [rpm]
C_{f0}	10	Friction coefficient
a_1	-88.67	Characteristic coefficient of pump head [m^{-5}s^2]
a_2	0	Characteristic coefficient of pump head [m^{-2}s]
a_3	43.15	Characteristic coefficient of pump head [m]

Table 5: Parameters of valves

Name	Value	Description
C_v^{max}	8005.42	Characteristic parameter of the valve [-]
ρ	998	Water density in the pump volume [kg/m^3]
k	1000	Singular pressure drop coefficient [Pa.s/m^3]
q_{min}	10^{-6}	Mass flow rate for feeding valve off [kg^3/s]

Table 6: Parameters of pipes

Name	Value	Description
Pipes		
ρ	998	Water density in the pump volume [kg/m^3]
g	9.80665	Gravity constant [m/s^2]
Δz	0	Inlet/outlet altitude change for pipes T_1, T_2, T_4 and $T-5$ [m]
Δz	30	Inlet/outlet altitude change for pipes T_6, T_8 [m]
k	25.36	Pipes T1, T2, T4 and T5 Pressure drop coefficient [Pa.s/m^3]
k	46.73 10^5	Pipes T6 and T8 Pressure drop coefficient [Pa.s/m^3]

A.2. Details of the Modelica model

A.2.1. Heat exchanger

The pressure drop between two control volumes for Equations (2) in the heat exchanger is given by:

$$\Delta P_{b,i} = c_{1,b} \cdot \frac{14423.2}{\rho_{b,i}} \cdot qm_{b,i}^{-0.097} \cdot qu_{b,i}^{2} \cdot \left(1472.47 + 1.54 \cdot \frac{M-1}{2} + 104.97 \cdot qm_{b,i}^{-0.25}\right) \tag{40}$$

where $c_{1,b}$ is the pressure drop correction coefficient and:

$$\begin{cases} qm_{b,i} = \dfrac{|q_{b,i}|}{\mu_{b,i} \cdot M} \\ qu_{b,i} = \dfrac{|q_{b,i}|}{M} \\ M = \dfrac{n-1}{2} \end{cases} \tag{41}$$

with n the heat exchanger plate number.

For the global heat exchanged between the both fluids and the wall (Equation 6), the heat exchange surface ΔS, and the global heat transfer coefficient K_I are given by:

$$\begin{cases} \Delta S = (n-2) \cdot S_p/(N-1), \\ K_I = (\overline{h}_h \cdot \overline{h}_c)/(\overline{h}_h + \overline{h}_c + \overline{h}_h \cdot \overline{h}_c \cdot \frac{e_m}{\lambda_m}), \\ \overline{h}_b = 11.245 \cdot |Nu_{b,i}|^{0.8} \cdot Pr_{b,I}^{0.4} \cdot \lambda_{b,I}. \end{cases} \tag{42}$$

where $\overline{h}_b$ is the convection heat transfer coefficient between the fluid and the wall. The Prandtl number $Pr_{b,I}$ and the correlation for the heat transfer $Nu_{b,i}$ (also called Nusselt number) are defined by:

$$\begin{cases} Pr_{b,I} = \mu_{b,I} \cdot Cp_{b,I}/\lambda_{b,I} \\ Nu_{b,i} = q_{b,i}/(\mu_{b,I} \cdot M) \end{cases} \tag{43}$$

In Equation (42) S_p is the branch section, e_m the metal wall thickness and λ_m the metal thermal conductivity.

A.2.2. Centrifugal pump

The resistant hydraulic torque C_h in Equation (26) is given by:

$$C_h = \frac{1}{r_h} \cdot \frac{q \cdot \Delta P}{\rho \cdot \omega} \tag{44}$$

where ΔP is the pressure increase between the pump inlet and outlet given by Equation (28), ρ the water density supposed here constant (incompressible fluid assumption), and r_h the pump hydraulic efficiency given by:

$$r_h = b_1 \cdot \frac{q^2}{\rho^2 \cdot R^2} + b_2 \cdot \frac{q}{\rho \cdot R} + b_3 \tag{45}$$

where $R = \frac{30\omega}{\pi \cdot N_{nom}}$ with N_{nom} the nominal angular velocity of the pump in rpm, and $b_i (i = 1, 2, 3)$ three characteristic constant coefficients.

The mechanical friction torque C_f in Equation (26) is given by:

$$C_f = \begin{cases} \text{sgn}(R) \cdot C_{f0} \cdot (1 - |R|) & \text{if } |R| < 1 \\ 0 & \text{otherwise} \end{cases} \tag{46}$$

where C_{f0} is a friction coefficient.

The pump head h_n in Equation (28) is given by:

$$h_n = a_1 \cdot \frac{1}{\rho^2} \cdot q \cdot |q| + a_2 \cdot \frac{1}{\rho} \cdot q \cdot R + a_3 \cdot R \cdot |R| \tag{47}$$

where as above $R = \frac{30\omega}{\pi \cdot N_{nom}}$ with N_{nom} the nominal angular velocity of the pump in rpm, and $a_i (i = 1, 2, 3)$ three characteristic constant coefficients.

A.3. Water pressure as function of specific enthalpy and density

To determine water pressure from specific enthalpy and density Algorithm 1 is applied on the density in terms of pressure and specific enthalpy table. Figure 33 shows the result in a 3D plot.

Algorithm 1 Calculate the water pressure from the density and the specific enthalpy

Require: ρ, h

$p_{min} = 0.00611657$; $p_{max} = 1000$;
$p_s = 100$; $\rho_s = \rho_s(p_s, h)$;
while $|\rho - \rho_s| > 0.0000001$ **do**
  $\rho_s = \rho_s(p_s, h)$
  if $\rho_s \geq \rho$ **then**
    $p_{max} = p_s$;
  else
    $p_{min} = p_s$;
  end if
  $p_s = (p_{min} + p_{max})/2$;
end while
$p = p_s$;

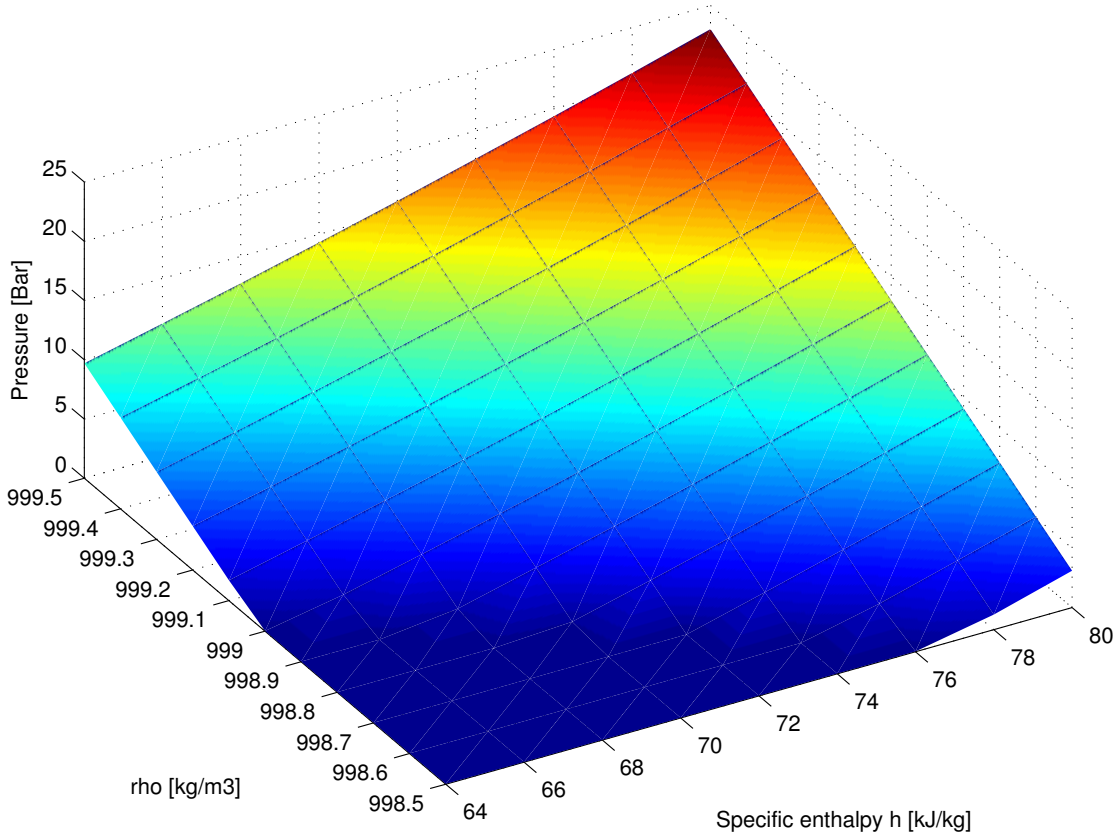

Figure 33: Pressure as a function of h and ρ.

A.4. Simulation results of the heat exchanger

A.4.1. Pressure drop approximation

Figure 34 shows a comparison between the Modelica model of the pressure drop at a boundary between two control volumes (ΔP_i from Equation (14)) and the approximation presented Equation (16) ($\Delta \bar{P}_i$). The simulations have been obtained by imposing the mass flow rate furnished by Dymola reference results on the R-field in the bond graph model.

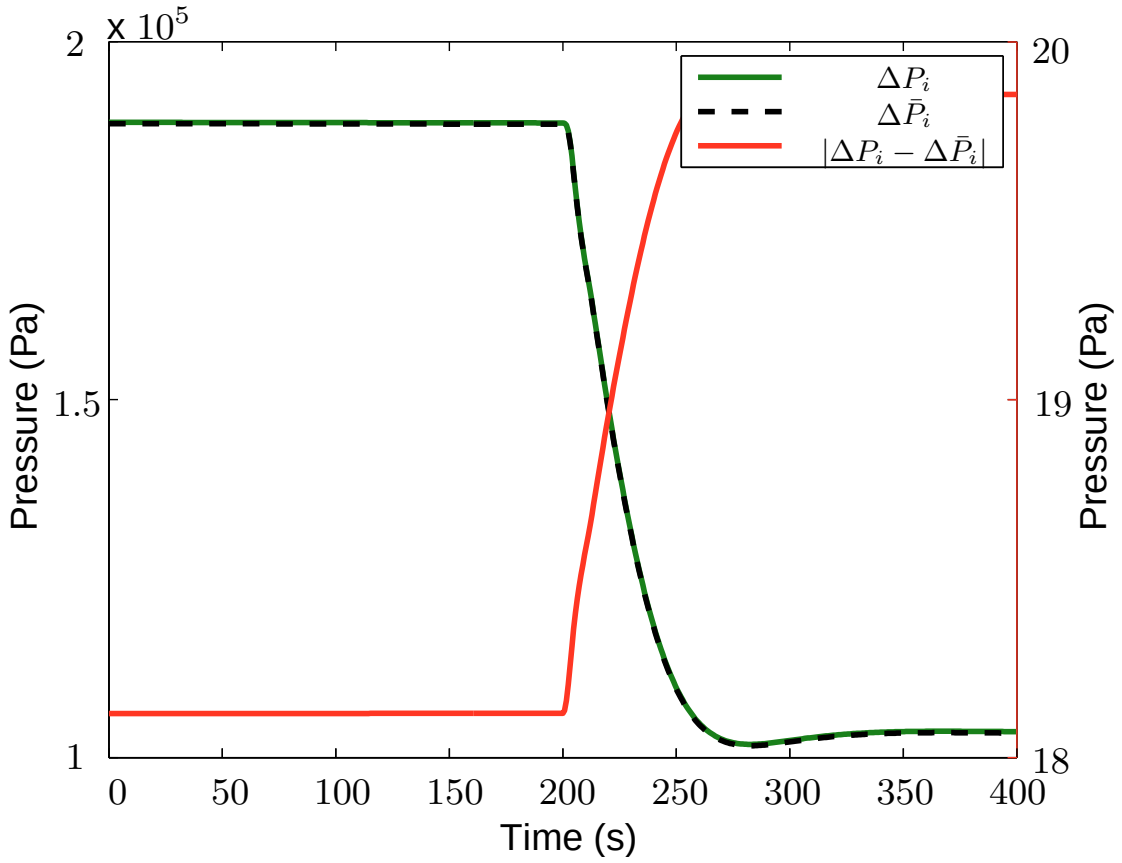

Figure 34: Comparison between the pressure difference

As a matter of verification Figure 35 shows the comparison between both mass flow rates in the hot branch obtained from Dymola and MS1[5] in which, q_i is calculated by Equation (17).

[5]MS1 is the acronym for Modelling System One, an interactive environment for modelling, simulation and analysis of non-linear dynamic modelled by bond graph systems [24]

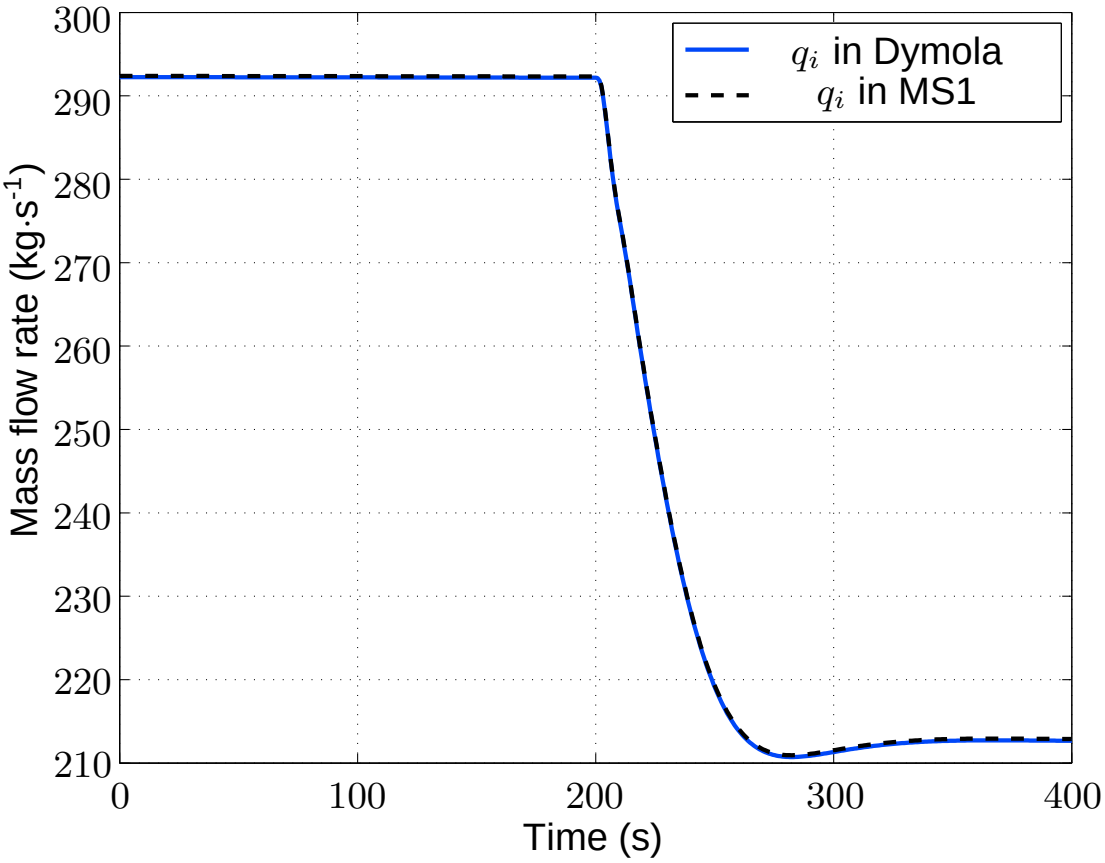

Figure 35: Comparison between both mass flow rates in Dymola and MS1

A.4.2. Simulation of the whole heat exchanger

As a matter of verification, a comparison of some simulations between the Dymola model and MS1 bond graph model of the whole heat exchanger composed of $N = 5$ lumps have been undertaken. The inputs of the models are the pressures and the temperatures at the exchanger boundaries furnished by the Dymola model.

The Modelica and the BG models were run for 400 seconds of simulation time. Figure 36 shows the pressures in the hot branch, where the black curves represent the pressures at the boundaries, the blue curves represent the pressures in the control volumes from the ThermoSysPro library in Dymola, and the dashed green curves represent the pressures from the C-elements in the bond graph model. From the comparison of these simulation results, the conclusion that can be made is that the both models have similar dynamic behaviors.

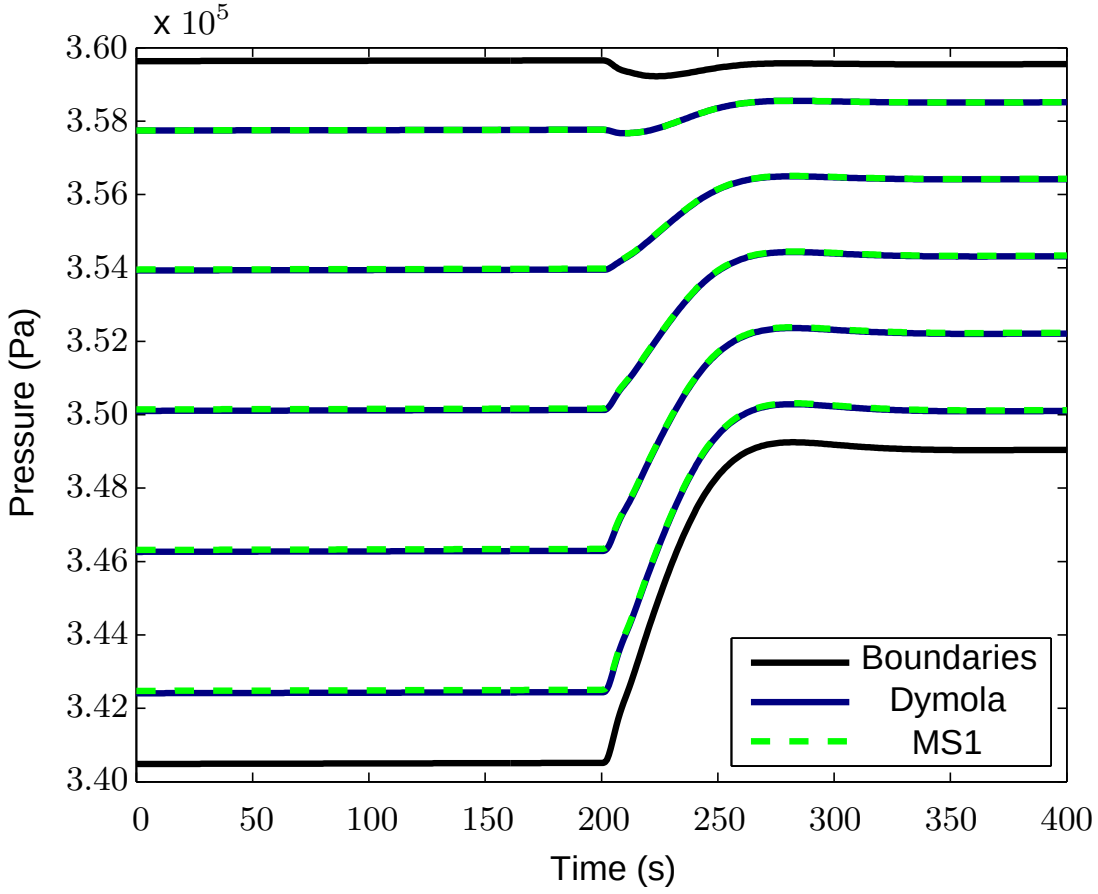

Figure 36: Comparison of bond graph model with Dymola model in the hot branch